

Intensified Warming and Aridity Accelerate Terminal Lake Desiccation in the Great Basin of the Western United States

Dorothy K. Hall^{1,2}, John S. Kimball³, Ron Larson⁴, Nicolo E. DiGirolamo^{5,2}, Kimberly A. Casey⁶
and Glynn Hulley⁷

¹Earth System Science Interdisciplinary Center, University of Maryland, College Park, MD
dkhall1@umd.edu

²NASA / Goddard Space Flight Center, Greenbelt, MD

³University of Montana, Missoula, MT john.kimball@mso.umt.edu

⁴Oregon Lakes Association, Klamath Falls, OR rlarson@ccountry.net

⁵Science Systems Applications, Inc., Seabrook, MD

⁶U.S. Geological Survey, Reston, VA kcasey@usgs.gov

⁷Jet Propulsion Lab, Pasadena, CA glynn.hulley@jpl.nasa.gov

Key Points

- MODIS data products provide a unique way to assess individual vulnerabilities of terminal lakes as temperatures rise in the US West
- Surface and air temperatures in the Great Basin are rising dramatically, with a sharp rise in the rate of increase observed beginning ~2011
- ET is generally low in the Great Basin, exacerbated by drought restrictions on surface evaporation, likely reinforcing regional warming

27 **Abstract**

28 Terminal lakes in the Great Basin (GB) of the western US host critical wildlife habitat and food
29 for migrating birds and can be associated with serious human health and economic consequences
30 when they desiccate. Water levels have declined dramatically in the last 100+ years due to
31 diversion of inflows, drought and climate change. Satellite-derived environmental science data
32 records (ESDRs) from the MODerate-resolution Imaging Spectroradiometer (MODIS) (snow
33 cover, evapotranspiration (ET) and land surface temperature (LST)), enable a unique approach to
34 evaluate the effects of aridification on terminal lakes and to study their individual vulnerabilities.
35 Surface and air temperatures in the GB are rising dramatically, with a sharp rise in the rate of
36 increase observed beginning around 2011, while the number of days of snow cover is declining
37 especially in the western mountainous part of the GB as exemplified in Mono Basin, California.
38 Rising temperatures coincide with fewer days of snow cover, a decrease of inflow to the lakes
39 and greater evaporation of water from the lakes. MODIS ESDRs show strong and statistically
40 significant increasing surface temperature (LST) in the GB, a reduction in the number of days of
41 snow cover, and mixed results in ET. ET declined slightly in the more arid parts of the GB due
42 to greater moisture restrictions to evaporation from extended drought, while ET increased in the
43 more-vegetated, wetter, mountainous northeastern parts as temperatures have risen. Severe and
44 costly ecological, human health and economic consequences are expected if the lakes continue to
45 decline as predicted.

46

47

Plain Language Summary

48 Terminal lakes in the Great Basin of the western US host critical wildlife habitat and food
49 sources for migrating birds and can be associated with costly human health and economic
50 consequences when they desiccate. Toxic minerals in the expanding lakebeds may become
51 airborne during windstorms, contributing to air pollution. Satellite data products (snow cover,
52 evapotranspiration and surface temperature) have enabled a unique understanding of the
53 dynamics of aridification in the Great Basin and associated effects on terminal lakes which are
54 usually saline. Surface temperature is rising dramatically, with a sharp rise in the rate of increase
55 observed beginning around 2011, while snow cover is declining especially in the western
56 mountainous part of the Great Basin as exemplified in Mono Basin, California.
57 Evapotranspiration has declined slightly in lower elevation parts of the Great Basin likely due to

58 a decrease in vegetation there, while it has increased in the wetter, mountainous eastern part as
59 temperatures have risen. Though we recognize that 21 years is not adequate for assessing trends,
60 it is clear that increasing temperatures, greater evaporation of lake water and decreasing number
61 of days of snow cover are contributing to desiccation of terminal lakes, with severe
62 environmental and human health consequences expected.

63

64 **Index terms**

65 0736 (snow), 0458 (limnology), 1855 (remote sensing), 1640 (remote sensing), 1818
66 (evapotranspiration), 0232 climate change: ecosystem health

67

68 **Key words**

69 Great Basin, terminal lakes, Lake Abert, Great Salt Lake, Mono Lake, drought, MODIS, snow
70 cover, evapotranspiration, land surface temperature

71

72

73 **1. Introduction**

74

75 A terminal lake has no outlets, losing water only through evaporation or groundwater seepage.
76 Terminal lakes have been shrinking worldwide, and water levels have declined in at least the last
77 100+ years, primarily due to increasing societal water demand exacerbated by periodic droughts,
78 lake and groundwater extraction, and climate change (Wurstbaugh et al., 2017). In the western
79 United States lakes have been losing water and shrinking dramatically, especially since the
80 current drought began around the year 1999 (Piechota et al., 2011).

81

82 In the Great Basin of the western US, streamflow from snowmelt in the mountains is the main
83 inflow to the terminal lakes which are typically shallow and have a large surface area. The
84 amount of water flow into the lake basins is affected by many variables such as: volume of snow
85 in the mountains, precipitation/drought and upstream diversions by humans. When the need for

86 water by humans increases during drought conditions, the need for more water flowing into the
87 lakes to maintain the health of the lakes also increases. Lower water levels are associated with
88 increased salinity, altered food webs and reduction of invertebrate food sources for shorebirds
89 and waterbirds.

90
91 Global climate models predict increasing temperatures and intensity of droughts in the western
92 US (Cook et al., 2015; McKenzie and Littell, 2017), with a projected increase in the fraction of
93 precipitation falling as rain vs snow, having the effect of decreasing snowpack water storage
94 (McCabe and Wolock, 2009; Frankson and Kunkel, 2016; Snyder et al., 2019; Williams et al.,
95 2022). Snowmelt is a more efficient mechanism for filling lakes than is rainfall (Berghuijs et al.,
96 2014). The reduction of snowfall and number of days of snow cover results in lower albedo and
97 greater absorption of solar radiation and heating at the Earth's surface (Déry and Brown, 2007;
98 Kumar et al., 2020). Additionally, a snowpack helps to reduce lake warming in summertime
99 because snowpack and water temperature are highly correlated in mountain lakes (Smits et al.,
100 2020).

101
102 Rapid surface warming on inland lakes has been documented for all parts of the globe (Zhang et
103 al., 2014; O'Reilly et al., 2015). For example, summer nighttime surface temperatures of large
104 inland water bodies increased at an average rate of 0.45°C/decade between 1985 and 2009 in
105 large lakes in California and Nevada (Schneider et al., 2009). In the latter part of the 20th
106 Century and the beginning of the 21st Century, the surface water of lakes warmed at an average
107 rate of 0.34°C/decade across the globe according to satellite measurements (O'Reilly et al.,
108 2015).

109
110 Terminal lakes play a critical but understudied role as sites of rare biodiversity and unique
111 chemical and ecological processes as feeding areas for migratory birds (Larson et al., 2016;
112 Senner et al., 2018; Haig et al. 2019). Migrating waterbirds rely on the network of terminal lakes
113 on their journeys through arid continental interiors (Donnelly et al., 2020) because the lakes can
114 provide a rich source of food and energy (e.g., brine shrimp and brine flies) for the birds (Oring
115 and Reed, 1997; Sorensen et al., 2020). Ultrasaline terminal lakes can also host

116 “extremophiles,” organisms that have provided invaluable information on the evolution of life
117 (e.g., Roberts, 2005).

118

119 Additionally, desiccating saline lakes can negatively impact human health when the dried
120 lakebed is exposed to wind erosion, reducing air quality (Zucca et al. 2021). Unconsolidated,
121 toxic (e.g., selenium, mercury, arsenic and other heavy metals) and hazardous (high-pH alkali)
122 substances are prevalent in the lakebed sediments. Windstorms can transport these toxic and
123 hazardous particulates for hundreds of kilometers.

124

125 Here, we evaluate specific factors that are driving the decline of Great Basin terminal lakes, with
126 a focus on three lakes that are widely separated within the Great Basin and are largely fed by
127 streams originating in snow-covered mountains: Lake Albert in Oregon, Great Salt Lake in Utah
128 and Mono Lake in California (Figure 1). The combination of consumptive water use, drought
129 and climate warming is jeopardizing the viability of these lakes (Larson et al., 2016; Wurstbaugh
130 et al., 2017; Haig et al., 2019; Donnelly et al., 2020; Hall et al., 2021).

131

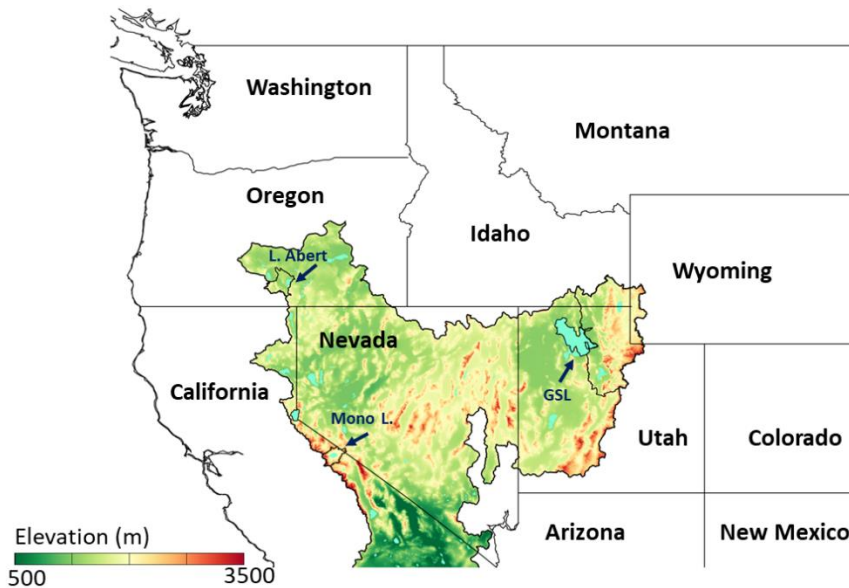
132 The drought in the Southwest US that has afflicted the region for over two decades is the driest
133 22-year period in the last 1,200 years (Williams et al., 2022). It is often referred to as a
134 megadrought which may be defined as a dry period lasting two decades or longer (Cook et al.,
135 2015; Williams et al., 2020 & 2022).

136

137 Only through the use of satellite data can we evaluate the regional changes that are affecting the
138 Great Basin under drought conditions. Using continuous, 21-year environmental science data
139 records (ESDRs) consisting of validated MODerate-resolution Imaging Spectroradiometer
140 (MODIS) standard data products: snow cover, evapotranspiration (ET) and land-surface
141 temperature (LST), along with ancillary data, we can gain an understanding of the individual
142 vulnerabilities of Great Basin terminal lakes and evaluate differences in the responses of each
143 lake to the current megadrought. Other satellite records are available with longer data records
144 suitable for assessing climate trends, but no other ESDRs provide comprehensive operational
145 land parameter records with a high level of precision enabled from continuous MODIS
146 operations on the Earth Observing System Terra satellite.

147

148



149

Figure 1. The boundaries of the Great Basin and the basins of Lake Abert, Oregon, Great Salt Lake (GSL), Utah and Mono Lake, California, in the western United States are outlined in black on this map of part of the western US. Arrows point to the study lakes. Only the effective area of the GSL basin, where all the streamflow enters the lake, is outlined. The digital-elevation model in the Great Basin was obtained from the USGS GTOPO30 digital-elevation model (USGS GTOPO30 DEM, 2019). Boundaries of the basins of Lake Abert, GSL and Mono Lake were obtained from shape files from the USGS National Map (2019).

157

158

159 2. Study Area and Background

160

161 The study area consists of most of the Great Basin of the western US and includes the basins of
 162 Lake Abert (2,753 km²), Great Salt Lake (39,732 km²) and Mono Lake (AKA Mono Basin,
 163 1,791 km²) (Figure 1). The Great Basin is a closed catchment of ~500,000 km² area located in
 164 Nevada, Utah, Oregon and California. This general area has been afflicted by enhanced
 165 adiabatic warming and resultant aridification since the end of the Pleistocene, but the rate of
 166 change has increased in at least the last few decades (Ficklin and Novik, 2017). Evaporation of

167 lake water in the Great Basin increased between 1985 and 2018 by ~+1.5 percent/decade because
168 of increasing air temperature and atmospheric vapor pressure deficit (Zhao et al., 2022). The
169 focus herein is on the time period from Water Year (WY) 2001 – 2021 which is also mostly
170 coincident with the timing of the current drought that began around 1999. The most severe
171 drought area is largely centered over the US Southwest, including much of the Great Basin
172 (Dannenberg et al., 2022; Williams et al., 2022).

173

174 2.1. Lake Abert, Oregon

175 Lake Abert (42.66°N, 120.23°W) is in the northwestern part of the Great Basin in south-central
176 Oregon (Figure 1). The lake gets most of its water from the Chewaucan River, which drains
177 snow-covered mountain ranges to the west of the lake, as well as small tributaries in the lower
178 part of the Chewaucan watershed (Larson and Larson, 2011; Larson and Eilers, 2014; Moore,
179 2016). However, upstream diversions are common. For example, it was documented by Phillips
180 and Van Denburgh (1971) that only about half of the flow of the Chewaucan River at Paisley,
181 Oregon, reached Lake Abert during the 50 years between 1913 and 1963.

182

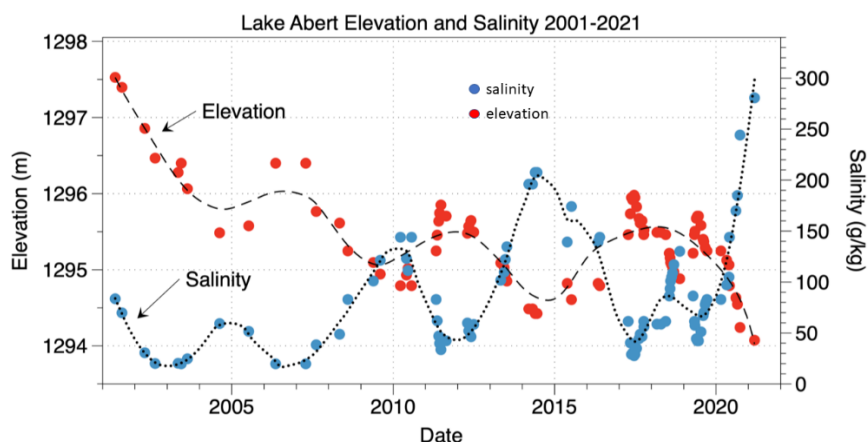
183 The highest “recent” surface-water elevation of Lake Abert was 1298.6 m in 1958 (Phillips and
184 Van Denburgh, 1971; Larson and Eilers, 2014). At the opposite extreme, Lake Abert was dry or
185 nearly dry during the Dust Bowl era in the 1920s and 1930s, reaching a low of ~1294.0 m in
186 1937 and again in June of 2014 (Phillips and Van Denburgh, 1971, Larson and Eilers, 2014), and
187 the surface-water elevation has continued to decline.

188

189 There is an inverse relationship between surface-water elevation and salinity in terminal lakes
190 (Figure 2). During the 21-year study period, salinity increased to a high of 250 g/kg in 2014 and
191 2015 in Lake Abert, but then decreased as the volume increased in 2017, then increased again
192 until it reached a new high of ~280 g/kg in 2021 as the volume decreased (Figure 2). In 2014
193 when the salinity was very high, the water turned bright red because of the presence of
194 ultrasaline-tolerant bacteria-like archaea microbes, such as *Halobacterium*, which contain a red
195 photosynthetic pigment (Larson et al., 2016).

196

197



198
 199 **Figure 2.** Lake Abert, Oregon surface-water elevations and estimated salinity in g/kg, WY 2001
 200 – 2021. Elevation data were obtained by volunteers reading a staff gage installed along the
 201 eastern shore of the lake. Salinity was measured from water samples using an optical
 202 refractometer. Because there were gaps in the salinity measurements, a second-order polynomial
 203 equation of salinity vs. elevation ($R^2 = 0.85$), was used to estimate salinity for every date on
 204 which there was an elevation measurement ($n = 47$). Some years show multiple elevations and
 205 salinities that were acquired in different seasons. Data used to create these plots are available in
 206 Table S3.

207

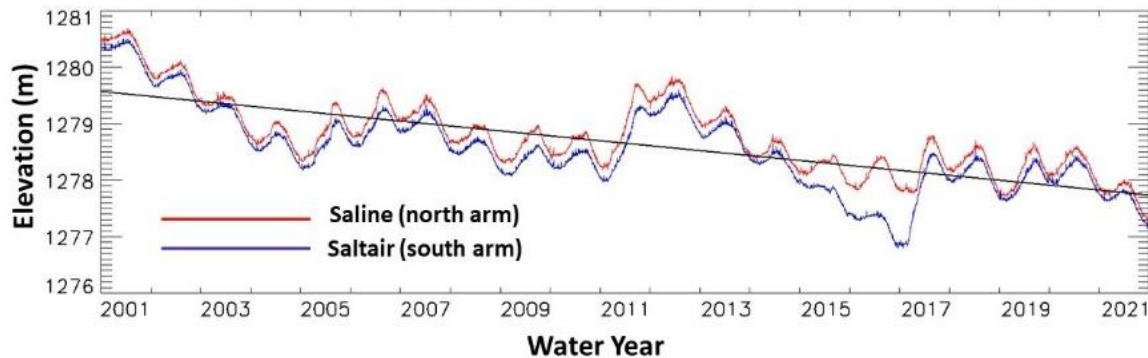
208

209 2.2. Great Salt Lake, Utah

210 Great Salt Lake (GSL) (41.12°N, 112.48°W), in the eastern part of the Great Basin (Figure 1), is
 211 the largest saline lake in North America though in the summer of 2019 the extent of the lake was
 212 only 2685 km² according to measurements using 30-m resolution Landsat data by Hall et al.
 213 (2021), and the lake has continued to shrink. Since the middle of the 19th Century, the volume
 214 and area of GSL have decreased by ~50 percent and the lake-water elevation has dropped by
 215 ~3.6 m with a concomitant increase in salinity (White et al., 2014a&b & 2015; Wurtsbaugh et
 216 al., 2017) (Figure 3). While upstream water diversions are the primary reason for the lowered
 217 lake levels since the mid-1800s, the continued desiccation of the GSL is exacerbated by
 218 increasing air and surface temperatures, and intensifying climate aridity, along with a trend
 219 toward earlier snowmelt and greater evaporation in the Wasatch and Uinta Mountains (Cook et
 220 al., 2004; Wurtsbaugh, 2017; Hall et al., 2021).

221

222



223

224 **Figure 3.** Daily mean surface-water elevations of the north and south arms of Great Salt Lake as
 225 measured at Great Salt Lake near Saline, UT (USGS Site Number 10010100) and Great Salt
 226 Lake at Saltair Boat Harbor, UT (USGS Site Number 10010000), respectively (USGS, 2022a).
 227 The black line represents the trend, in m/yr, derived from an average of the elevations from the
 228 north and south arms of the lake (USGS, 2022a). Extended from Hall et al. (2021).

229

230

231 The waters of the Bear, Jordan and Weber rivers, the primary tributaries to GSL, originate in the
 232 snow-dominated Wasatch and Uinta mountains to the east and northeast of the lake. Every year,
 233 an estimated 3.3 trillion liters of water are diverted from the streams feeding the GSL (Derouin,
 234 2017) to support agricultural, industrial and municipal water uses in the basin. The upstream
 235 diversions, warmer temperatures, reduced snow cover and greater evaporation in the GSL basin
 236 to the east of the lake (32,251 km²), from which nearly all the inflow occurs (the effective area of
 237 the GSL basin), are contributing to the ongoing trend toward lower water levels (Hall et al.,
 238 2021).

239

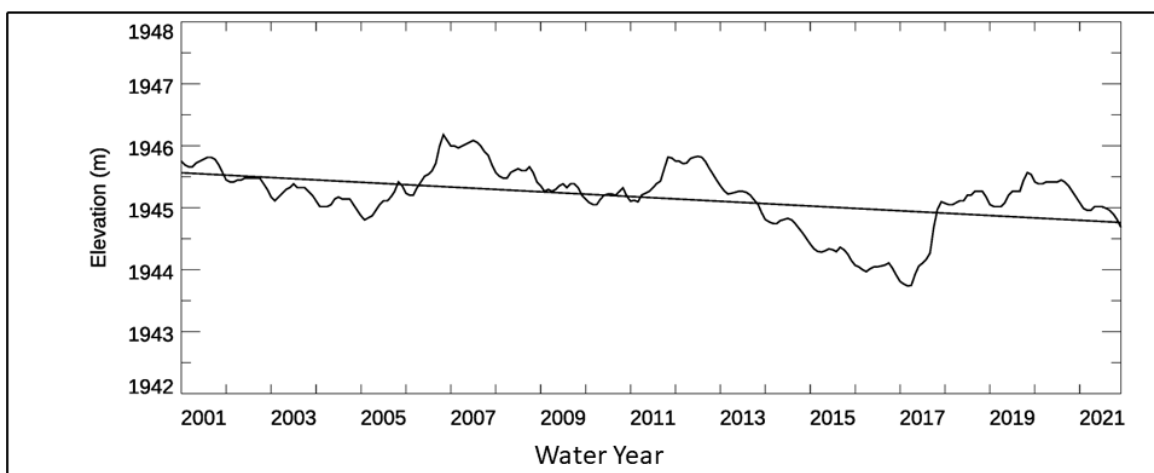
240 As the volume of the lake decreases and more lakebed is exposed, there are serious
 241 environmental and potential human health consequences as discussed further in the Discussion
 242 section. GSL is an important stopover for millions of migratory water birds (Audubon, 2022),
 243 however, the sustainability of the birds' primary food sources, brine shrimp and brine flies, is
 244 jeopardized when the salinity increases to levels that are toxic to the invertebrates.

245

246 2.3. Mono Lake, California

247 Mono Lake (37°58'N, 119°08'W) is located on the western edge of the Great Basin, on the
 248 eastern side of the Sierra Nevada Mountains in California (Figure 1). The highly alkaline lake
 249 (Nielsen and DePaolo, 2013) provides habitat and food for numerous water birds, most of which
 250 are migratory. Many of these birds feed on the unique *Artemia monica* brine shrimp that are
 251 endemic to Mono Lake (Mason, 1966; Conte et al., 1988). While most terminal lakes in the
 252 Great Basin are located at lower elevations and are shallow, Mono Lake, one of the highest large
 253 terminal lakes in North America at 1944.5 m (as of July 2022 (MLC, 2022 a & b), is relatively
 254 deep (up to ~48 m) (Melack, 1983; Vorster, 1985), but still declining; it was 51 m deep in the
 255 1960s (Mason, 1966).

256
 257
 258



259
 260 **Figure 4.** Plot of daily lake elevations of Mono Lake, WY 2001 – 2021. Source: Mono Basin
 261 Clearinghouse (MBC, 2022).

262
 263
 264 Most of the inflow to Mono Lake originates from runoff from three major perennial streams:
 265 Rush Creek, Lee Vining Creek and Mill Creek, contributing ~53 percent, ~33 percent, and ~14
 266 percent of the total runoff, respectively (Romero and Melack, 1996; Ficklin et al., 2013; Vorster,

267 1985). The lake itself does not receive much rainfall or snowfall directly because of its position
268 in the rain shadow of the Sierra Nevada Mountains (NRC, 1987).

269
270 Beginning in late 1940, some tributaries to Mono Lake were diverted by the Los Angeles
271 Department of Water and Power to augment the water supply of the City of Los Angeles, ~500
272 km to the south. As a result, by January of 1982, the lake surface elevation dropped ~14 m, to
273 1942 m, the lake volume had decreased by 45 percent (MBC, 2022) Ficklin et al., 2013; Herbst,
274 2014), and the salinity doubled (MLC, 2022a&b). The lower water levels in Mono Lake have
275 had indirect negative effects, such as reduction of habitat and decline of food sources for
276 migratory birds.

277
278 Because the viability of Mono Lake is impacted by upstream diversions, legislation was enacted
279 in 1994 to reduce the impact by allowing the lake level to rise to 1948 m. However, that
280 elevation has not yet been achieved, partly due to the ongoing drought (Herbst, 2014).

281

282

283 3. Data and Methodology

284

285 In this work we use MODIS satellite data products and meteorological station data to assess the
286 changes and trends in snow cover, snow-water equivalent (SWE), evapotranspiration (ET), and
287 daytime and nighttime land surface temperature (LST) and air temperature over the 21-year
288 study period (WY 2001 – 2021) for the western US with a focus on the Great Basin as a whole
289 and separately for the basins of Lake Abert, GSL and Mono Lake. Surface-water elevations of
290 the lakes were derived from various sources and the surface areas of Lake Abert, GSL and Mono
291 Lake were measured using remotely-sensed imagery and data products (described below). These
292 geophysical parameter variables are considered essential climate variables that are key to
293 tracking and understanding temperature, precipitation and hydrological change through time.

294

295 3.1. MODIS satellite data products

296 The NASA standard data products used in this work: snow cover, land surface temperature
297 (LST) and evapotranspiration (ET), are derived from the MODIS sensor on the Terra satellite.
298 These complementary data products are well characterized and validated and cover key elements
299 of the near-surface climate, water and energy budgets. The spatial resolutions of the products are
300 well suited for investigations of the heterogeneous landscape. Data are available beginning 24
301 February 2000, and extend to the present, except during short-term outage periods caused by
302 spacecraft maneuvers, temporary software or instrument issues or upgrades (LDOPE, 2022).
303 The snow cover, LST and ET products have been validated at Stage 2. Stage 2 validation means
304 that “Product accuracy is estimated over a significant (typically >30) set of locations and time
305 periods by comparison with reference *in situ* or other suitable reference data.” See CEOS-LPV
306 (2022) for a detailed description of validation stages.

307
308 First we developed maps of mean annual snow cover, ET and LST for the Great Basin for the
309 study period (WY 2001 – 2021). To develop a snow-cover map from MOD10A1F, only
310 ‘persistent’ snow cover was mapped. Persistent snow cover in a pixel is defined herein as having
311 at least seven consecutive days of snow cover in each of the 21 years, thus eliminating snow that
312 might be present for less than one week in some or all years. In this work non-persistent snow
313 cover is termed ‘ephemeral.’ Mean annual ET was calculated from all available 8-day
314 MOD16A2GF products during the study period. LSTs from MOD21A1D and MOD21A1N for
315 each non-cloudy pixel in each day of the study period were averaged to get a daily mean LST in
316 each non-cloudy pixel. Daily data were then averaged for the study period to create the mean
317 LST map.

318
319 **3.1.1. Snow cover.** The MODIS Terra cloud-gap filled normalized-difference snow index
320 (NDSI) 500-m resolution snow-cover map product, MOD10A1F (Hall and Riggs, 2020), from
321 MODIS Collection 6.1 (C6.1) was used to provide a daily ‘clear-sky’ snow map of the Lake
322 Abert, GSL and Mono Lake basins and to calculate the number of days (#days) of snow cover
323 for each pixel for every available day during the study period within Great Basin as a whole and
324 also for each of the three lake basins individually. Uncertainties in the snow-cover decisions in
325 the cloud-gap filled maps that relate to the gap-filling methodology depend in part on the age of
326 the observation, i.e., the number of days since the last cloud-free observation in each pixel, and

327 are discussed in detail elsewhere (Hall et al., 2010 & 2019; Riggs et al., 2018). MOD10A1F was
328 developed and produced at Goddard Space Flight Center and is distributed by the NASA
329 Distributed Active Archive Center (DAAC) at the National Snow and Ice Data Center (NSIDC)
330 in Boulder, Colorado, and may be downloaded from NSIDC.

331
332 **3.1.2. Evapotranspiration.** The 500-m resolution C6.1 NASA standard evapotranspiration (ET)
333 Gap-Filled 8-Day Level 4 Global 500m product, MOD16A2GF (Running et al., 2021), was used
334 to develop per-pixel ET maps in the Great Basin for the study period. ET is the sum of water
335 vapor fluxes from soil evaporation, wet canopy evaporation and plant transpiration from the dry
336 canopy surface; the MOD16 algorithm uses daily meteorology reanalysis from the NASA Global
337 Modeling and Assimilation Office Goddard Earth Observing System Forward Processor along
338 with 8-day remotely sensed vegetation property dynamics from MODIS as key inputs (Mu et al.,
339 2011). The MOD16 algorithm uses the Penman-Monteith model which is well suited for semi-
340 arid dryland regions owing to explicit representation of vegetation canopy stomatal and surface
341 restrictions to evaporation (Zhang et al., 2016).

342
343 First we used the 8-day total ET values to calculate a total annual ET value in mm for each of the
344 21 years of record; these data were then used to calculate the average annual ET for the study
345 period. We also used the total per-pixel ET value in each water year to calculate the per-pixel
346 change in ET (in mm). The MOD16 algorithm and ET product has been extensively validated
347 over a global domain spanning multiple data years and diverse climate and vegetation
348 conditions; the ET product accuracy and performance is comparable to daily ET measurements
349 obtained from in situ tower eddy covariance measurements (Mu et al. 2011; Bajgain et al., 2020;
350 Brust et al., 2021). MOD16A2GF data products may be downloaded from the NASA EOSDIS
351 Land Processes DAAC at the EROS Data Center in Sioux Falls, South Dakota.

352
353 **3.1.3. Land surface temperature (LST).** MODIS LST C6.1 data products, MOD21A1D
354 (daytime) and MOD21A1N (nighttime) (Hulley and Hook, 2021a&b; Hulley et al., 2017), are
355 used to map daytime and nighttime LST trends in each pixel in the Great Basin at 1-km
356 resolution. The mean daily LST in the Great Basin was derived by averaging the daily daytime
357 (MOD21A1D, 10:30 AM) and nighttime (MOD21A1N, 10:30 PM) LST on a per pixel basis. To

358 fill in the gaps caused by clouds, we used a 3rd order cubic polynomial of the LST data to
359 develop basin trend plots.

360
361 We also used C6.1 MOD21C3 5-km resolution monthly LST products to look at day/night
362 differences in LST trends in the Great Basin for the study period. The monthly gridded product
363 is computed by averaging the best quality data in the MOD21A1D (daytime) and MOD21A1N
364 (nighttime) gridded data.

365
366 Additionally, we used the C6.1 LST products to measure the surface temperature trends of GSL
367 and Mono Lake. For GSL, we developed a water mask consisting of pixels representing a
368 minimum extent of the lake for the study period, to ensure that we would capture only water
369 pixels even in drier years. For Mono Lake we used the USGS dynamic surface-water extent
370 (DSWE) mask (USGS, 2022b) to determine the ‘high confidence water’ of each lake for each
371 year during the study period (see next section for a further description of the DSWE). We then
372 measured LST only for the water pixels in each year. We did not measure the LST trend of Lake
373 Abert because the lake was nearly desiccated in 2014, 2015 and 2021. There was not adequate
374 water in the lake in those years in which to measure LST with confidence. All MODIS LST data
375 products may be downloaded from the NASA Earth Observing System Data Information System
376 Land Processes DAAC at the EROS Data Center in Sioux Falls, South Dakota.

377

378 **3.2. Temporal changes in areal extent of the study lakes**

379 Landsat Collection-2 atmospherically-corrected Surface Reflectance data products, were used to
380 measure the length and width of Mono Lake on 30 July 2001 using Landsat-7, and on 24 July
381 2022 using Landsat-9. We then compared those results with results from Mason (1966) who
382 measured Mono Lake in the early-to-mid 1960s (the exact date of the measurements is not
383 known). We also used Landsat-8 Operational Land Imager (OLI) 30-m resolution imagery to
384 measure the areal extent of Great Salt Lake in 2020 and 2021. Interpretation was based on
385 human visual analysis using spatial geographic software when there was no computer-assisted
386 binary (land/water) classification to delineate lake extents. The details of the Landsat scenes that
387 were used in this work are provided in Table S1.

388

389 The Landsat Collection 2 (C2) Level-2 Dynamic Surface Water Extent (DSWE) product (USGS,
390 2022b) was used to determine the surface water area of the study lakes to plot the changes in
391 areal extent. The Landsat DSWE provides high temporal, moderate spatial resolution long-term
392 data on terrestrial surface inundation using the Landsat at-surface reflectance product and a
393 digital elevation model as inputs (Jones, 2019). A DSWE map was selected from fall scenes and
394 used to calculate the extent. However, in 2007, good quality data were not available in the fall,
395 so a map from August was used instead. The measurements of areal extent were used to plot
396 extent changes of each lake.

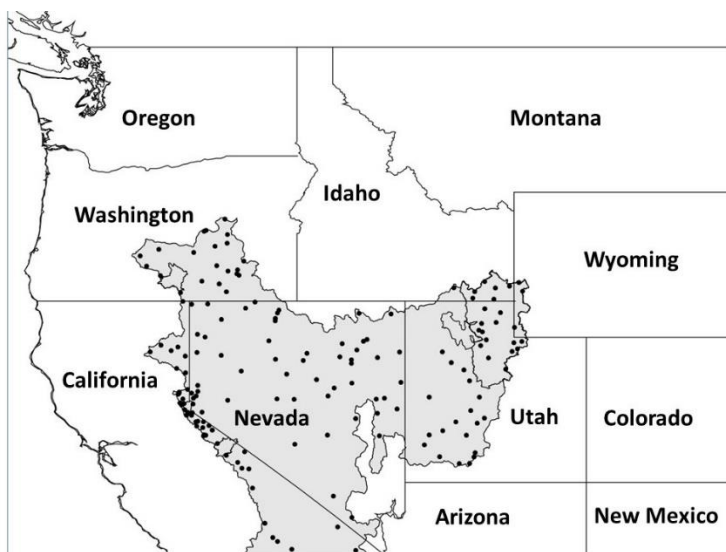
397

398 **3.3. Meteorological station data**

399 We calculated a mean-daily air temperature of the Great Basin for WY 2001 – 2021. There are
400 292 NOAA meteorological stations located within the boundaries of the Great Basin; all daily
401 minimum, T_{min}, and maximum, T_{max}, air temperatures, were downloaded, however we did not
402 use data from all 292 stations. Data from a station was accepted only if it had >272 days in
403 which *both* T_{min} and T_{max} were available for at least 20 years of the 21-year study period.
404 After filtering according to the restriction above, 164 stations were selected for use (Figure 5).
405 Furthermore, for a day to be used in our calculation of mean daily air temperature, 80 percent or
406 more of the 164 stations had to report T_{min} and T_{max} on that day. Because the stations are not
407 evenly distributed within the Great Basin, the resulting ‘mean-daily air temperature’ calculation
408 is only an approximation of the actual mean air temperature on any given day, and the mean-
409 daily air temperature of the study period in the Great Basin. The air temperature data used in this
410 study were obtained from NOAA National Centers for Environmental Information (NCEI,
411 2022).

412

413



414
 415 **Figure 5.** Black dots show locations of NOAA meteorological stations (total = 164) that were
 416 used to develop mean-daily average air temperatures in the Great Basin. Air temperature data
 417 were obtained from NOAA National Centers for Environmental Information (NCEI, 2022).

418
 419

420 3.4. Snow-water equivalent (SWE) from SNODAS and SNOTEL

421 Snow-water equivalent (SWE) data were obtained from NOAA's National Weather Service
 422 (NWS) National Operational Hydrologic Remote Sensing Center (NOHRSC) SNOw Data
 423 Assimilation System (SNODAS), which has provided an estimate of daily SWE for the western
 424 United States and elsewhere since 2003. SNODAS procedures assimilate satellite-derived,
 425 airborne, and ground-based observations of snow-covered area and SWE, then provide estimates
 426 of SWE and other parameters in support of hydrologic modeling and analysis (Carroll et al.,
 427 2001; NOHRSC, 2004; SNODAS, 2022). Daily SWE from SNODAS is generated on a 1-km
 428 spatial resolution grid and was analyzed for the Great Basin for WY 2004 – 2021.

429
 430 SWE data from the SNOTEL network were downloaded from the Natural Resources
 431 Conservation Service, National Water and Climate Center (NRCS, 2022). Two SNOTEL sites
 432 were selected within or as close as possible to the basins of Lake Abert and GSL, then averaged
 433 for each pair for each basin. Only one SNOTEL station was found close enough to Mono Basin
 434 to be useful. The stations are listed in Table S2.

435

436 3.5. Surface-water elevation

437 To determine the lake surface-water elevations, we used data from various sources. For Lake
438 Abert, elevation data were obtained by reading a staff gage. For GSL, USGS Water Information
439 System data were used (USGS, 2022a). For Mono Lake, data from the Mono Basin
440 Clearinghouse (MBC, 2022) were used.

441

442

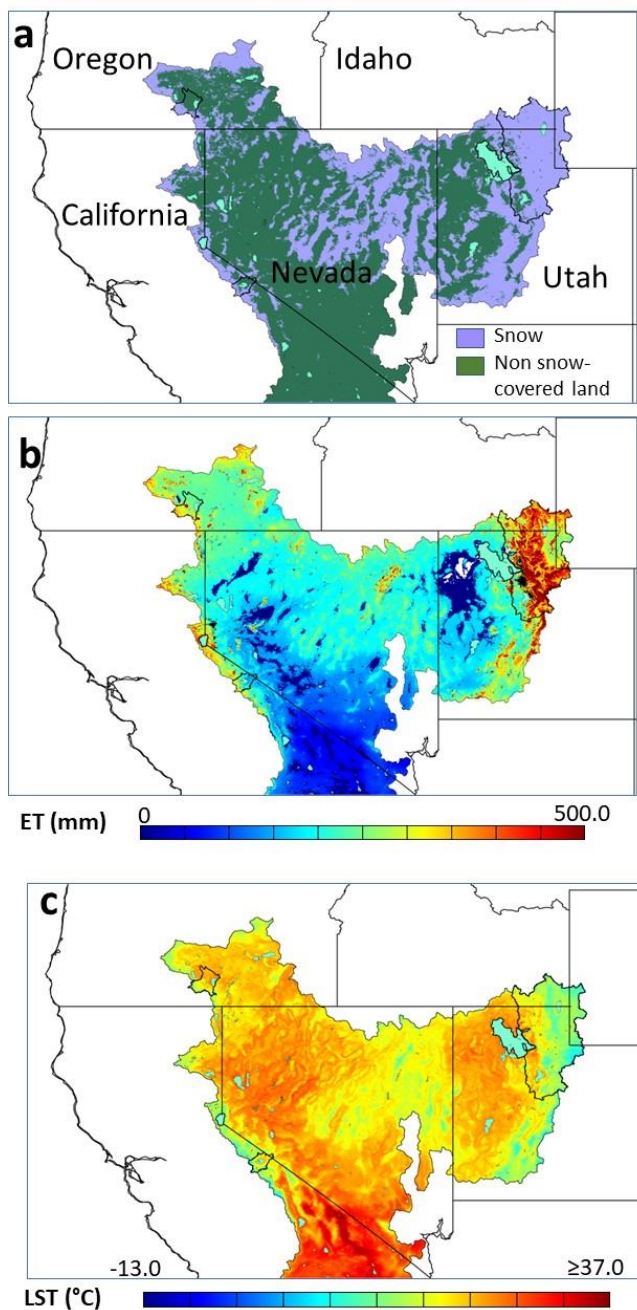
443 4. Results

444

445 There is quite a bit of complementary information in the MODIS maps of snow cover, ET and
446 LST in the Great Basin (Figure 6), and in their associated trends over the broader western US
447 (Figures S1, S2 and S3). Lower LSTs generally correspond with persistent snow cover and with
448 higher ET rates, especially in mountainous areas on the periphery of the Great Basin (Figure 6).
449 In the Great Basin as a whole and specifically in the Lake Abert, GSL and Mono Lake basins,
450 there is a trend toward fewer days of snow cover and lower SWE, mixed (both increasing and
451 decreasing) trends in land surface ET, and strongly increasing daytime and nighttime LST. In
452 the following paragraphs we discuss trends in snow cover, ET and LST in the Great Basin, and
453 regional differences in their apparent response to drought conditions in different parts of the
454 Great Basin, as seen in the three lake basins for the study period.

455

456



457
 458 **Figure 6 a, b, c.** MODIS-derived maps of the Great Basin in the western United States, 2001 –
 459 2021; basins of Lake Abert, Oregon, Great Salt Lake, Utah and Mono Lake, California are
 460 outlined in black. Some of the larger lakes within the Great Basin are shown in aquamarine. **a)**
 461 Mean annual 'persistent' snow cover from MOD10A1F; **b)** mean annual evapotranspiration from
 462 MOD16A2GF; **c)** mean annual land-surface temperature from MOD21A1D & MOD21A1N.
 463
 464

465 Outside of the Great Basin, in parts of Montana and Wyoming, there are areas indicating an
466 *increasing* number of days (#days) of snow cover (Figure S1) especially in northern Montana,
467 and roughly in the same location as the trends of *decreasing* LSTs seen in Figures S1 and S2.
468 ET also tends to be reduced over much of the interior Great Basin and California, where the
469 extended drought has severely restricted water supplies available to support ET and vegetation
470 growth (Dannenberg et al., 2022). Trends of decreasing ET from plants and soil in the Great
471 Basin and in California contrast with moderate increases in ET elsewhere as seen in Figure S3.
472 In the Sierra Nevada Mountains in eastern California, the number of days of snow cover are
473 declining in much of the same area that shows the greatest decline in ET (Figures S2 and S3).

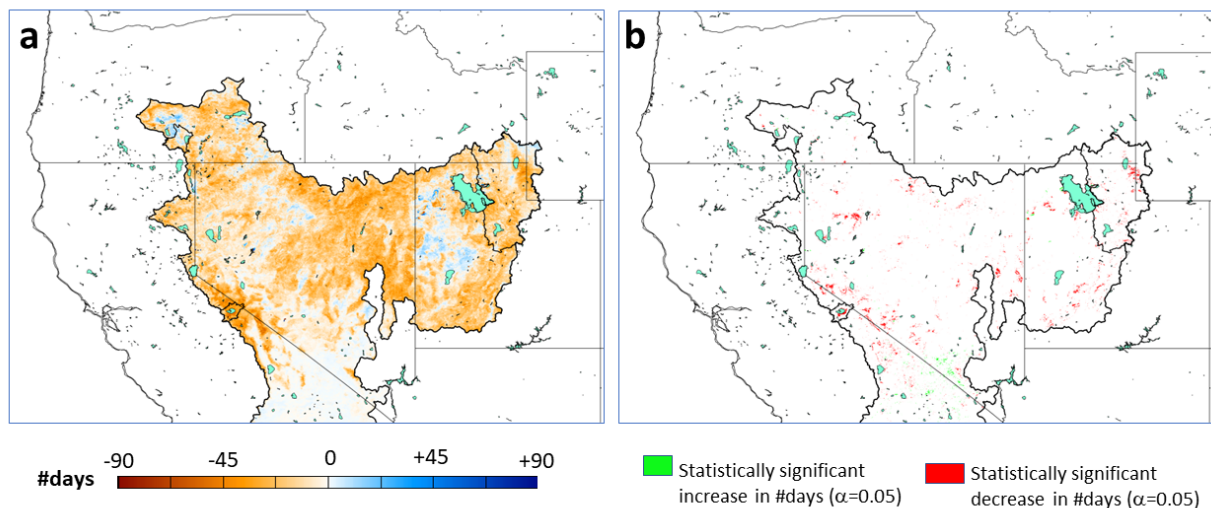
474

475 4.1. Trends in snow cover and snow-water equivalent (SWE) for the Great Basin

476 For the Great Basin as a whole, there is an average of 12.4 fewer #days of snow cover (Figure
477 7a) over the 21-year period. The decline in snow cover is widespread, though most pixel trends
478 are not statistically significant ($\alpha=0.05$) (Figure 7b). In the areas of persistent snow cover as
479 defined in Section 3.1 (see Figure 6a) there was an average of 18.4 fewer #days of snow over the
480 study period. The lack of statistical significance is likely because interannual (climate)
481 variability in snow cover is much larger than the long-term trend, which contributes to lower
482 trend significance. However, the widespread trend pattern of fewer #days of snow cover is
483 consistent with rising temperatures and declining lake levels. Areas where there was a lack of
484 change and even weakly increasing in #days of snow cover in central to western Utah (white to
485 light blue pixels in Figure 7a) are located at lower elevations (Figure 1), where snow cover is not
486 persistent.

487

488



489
 490 **Figure 7 a & b.** a) Change (per pixel) in number of days of snow cover for the Great Basin
 491 derived from the MODIS standard snow-cover product, MOD10A1F. b) Green or red pixels
 492 within the boundary of the Great Basin show statistical significance at $\alpha=0.05$. Within the Great
 493 Basin, the boundaries of the basins of Lake Abert, GSL and Mono Lake are outlined in black.
 494 Some of the larger lakes in the western US are shown in aquamarine. A water mask shows large
 495 lakes and reservoirs both inside and outside the study domain.

496
 497
 498 In all three lake basins there are declines in #days of persistent snow cover (Figure 8a-f). This
 499 decline is particularly notable in Mono Basin with an average of 28.4 fewer days of snow cover
 500 (Table 1). Though most of the pixels in the basins do not show statistically significant trends in
 501 #days of snow cover, there are some clusters of pixels showing statistically-significant trends
 502 ($\alpha=0.05$) in Mono Basin (Figure 8f), and in the GSL basin especially south and east of the lake
 503 (Figure 8d).

504
 505
 506 **Table 1.** Change* in #days of persistent snow cover, in each of the three lake basins, WY 2001-
 507 2021, derived from MOD10A1F.

508

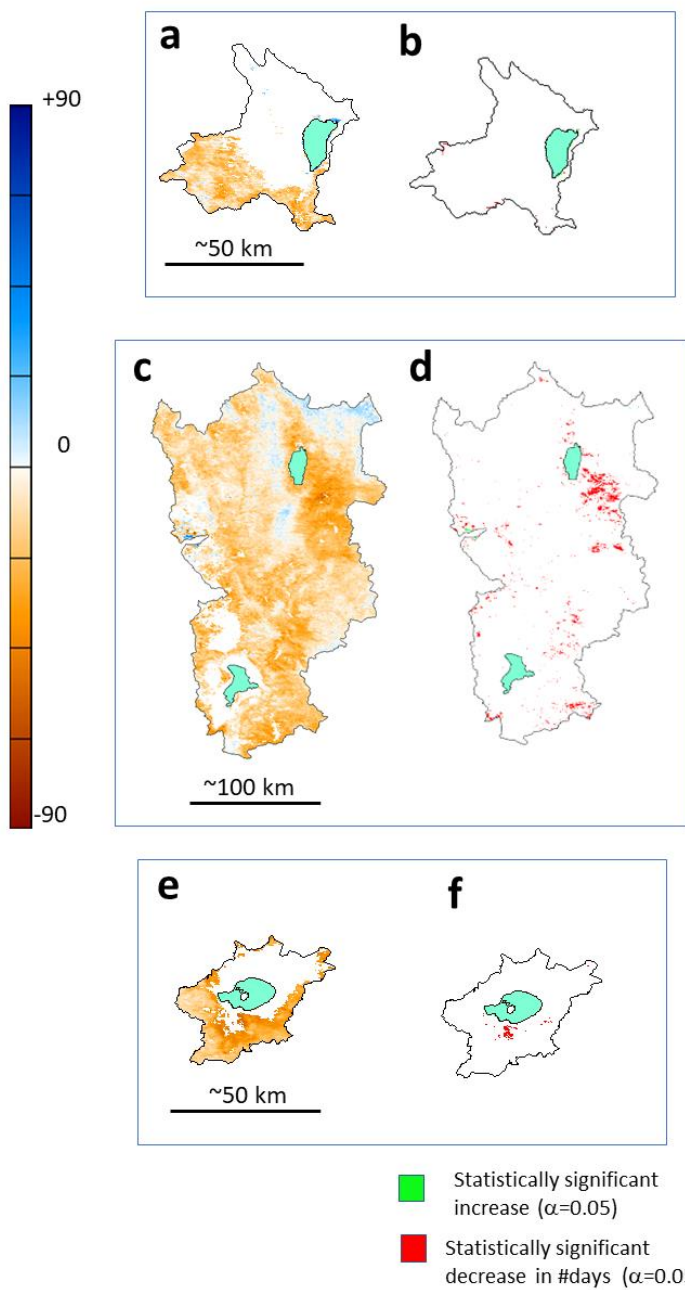
	Lake Abert	Great Salt Lake	Mono Lake

#days	-14.6	-14.1	-28.4
-------	-------	-------	-------

509 *Derived from the end points of the trend lines.

510

511



512

513 **Figure 8 a-f.** Change (per pixel) in number of days (#days) of 'persistent' snow cover (as
 514 defined in Section 3.1) in the basins of a) Lake Abert, c) Great Salt Lake and e) Mono Lake,

515 derived from the MODIS standard snow-cover product, MOD10A1F. Statistical significance
516 ($\alpha=0.05$) maps of trends in #days of snow cover for **b)** Lake Abert, **d)** Great Salt Lake, and **f)**
517 Mono Lake are also shown.

518

519

520 The total mean change in SWE (2004 – 2021), determined from SNODAS data (SNODAS,
521 2022) in the Great Basin was found to be -3.7 mm and is statistically insignificant. Larger
522 changes in SWE were observed at the SNOTEL stations that are associated with the three lake
523 basins (listed in Table S2).

524

525 Lake Abert and Mono Lake basins show 21-year declines in SWE at the SNOTEL stations, with
526 slopes of -0.4 cm/yr (mean SWE from the Strawberry and Summer Rim SNOTEL sites) to -
527 0.2 cm/year (SWE from the Virginia Lakes SNOTEL site), respectively. Though there is an
528 increase in SWE (0.5 cm/yr) from an average of the Franklin and Tony Grove SNOTEL sites of
529 the GSL basin, the historical record from 1979 – 2021 shows a general SWE decline in all three
530 basins.

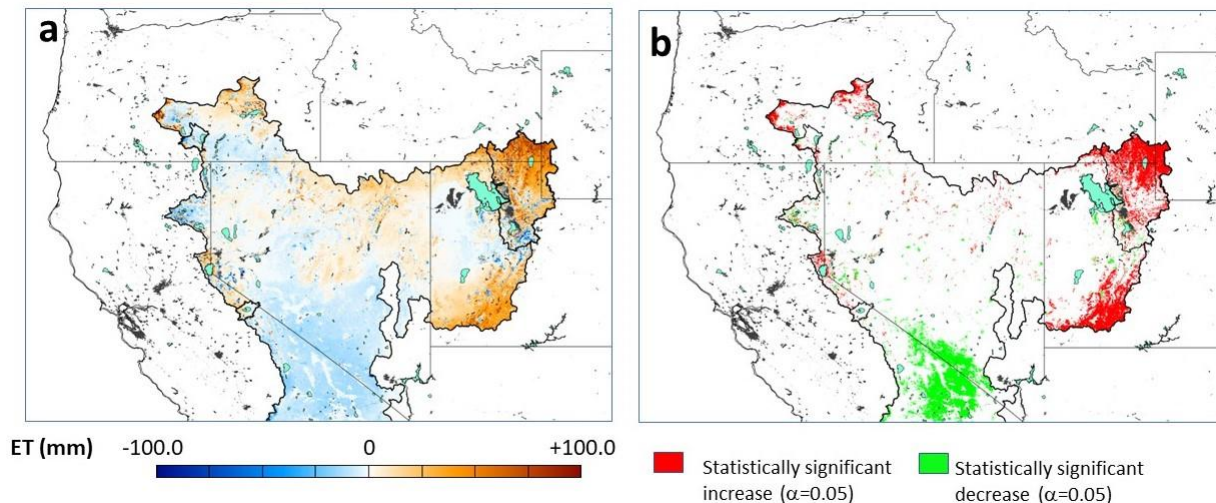
531

532 4.2. Changes in ET

533 Results derived from the MOD16A2GF standard ET data products show weak but insignificant
534 trends of decreasing ET in much of the Great Basin (Figure 9a&b) except in the eastern part
535 where the ET increased over the study period. The mean change in ET in the Great Basin over
536 the 21-year record was only +3.1 mm, but with much larger spatial variability ranging up to
537 +100 mm in the eastern Great Basin, contrasting with a decrease in ET in the southern and
538 western regions. Most of the trends in ET are not statistically significant ($\alpha=0.05$) with the
539 exception of the positive trends in the higher elevation areas of the Wasatch Mountains in the
540 eastern Great Basin (Figure 9b). Widespread neutral or slightly-negative ET trends largely occur
541 in lower elevation areas characterized by sparse dryland vegetation.

542

543



544
 545 **Figure 9 a & b.** Total change in evapotranspiration (ET) in mm, WY 2001-2021 for the Great
 546 Basin derived from the MODIS standard ET product, MOD16A2GF. The larger lakes are shown
 547 in aquamarine. There was no ET retrieval in the few pixels that are colored dark grey. A water
 548 mask shows large lakes and reservoirs both inside and outside the study domain.

549
 550
 551 There was a small and generally insignificant change in ET in the basins of Lake Abert and
 552 Mono Lake, but an overall increase in ET in the GSL basin (Figure 9a&b and Table 2). Lake
 553 Abert basin showed a mean ET decrease of -5.2 mm over the period, with some pixels in the
 554 basin showing statistical significance ($\alpha = 0.05$) for increasing and decreasing ET, particularly in
 555 the southern half of the basin (Figures 9a&b). For the GSL basin, there was a mean ET increase
 556 of +28.1 mm, with 29.4 percent of basin pixels showing a statistically significant positive trend
 557 ($\alpha = 0.05$), mainly in the northern half of the basin, and only 1.1 percent of pixels showing a
 558 statistically-significant negative ET trend. For Mono Basin, there was also little change in ET
 559 over the study period, with a mean change of +3.3 mm. Most of the pixels showed weak positive
 560 or negative changes that are statistically insignificant ($\alpha = 0.05$).

561
 562
 563 **Table 2.** Mean total change* in ET in mm, WY 2001 – 2021, in the basins of Lake Abert, Great
 564 Salt Lake and Mono Lake, derived from MOD16A2GF.

565

Lake Abert	Great Salt Lake	Mono Lake
-5.2	+28.1	+3.3

566 *Derived from the end points of the trend lines.

567

568

569 4.3. Changes in LST and air temperature in the Great Basin

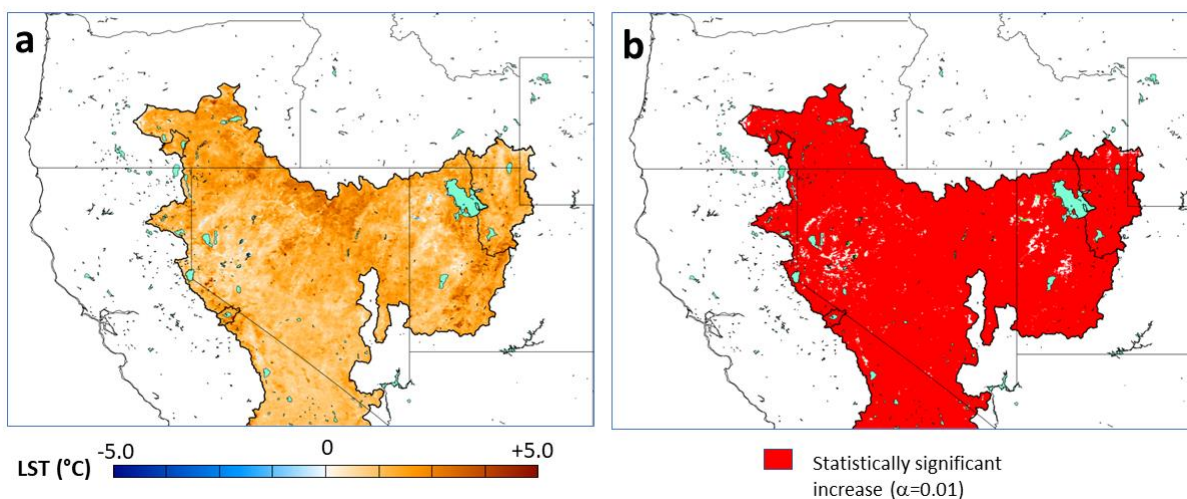
570 In Figure 10a, strongly increasing LST is evident, with a rate of increase of 1.0 °C/decade and a
 571 total mean increase of 2.1°C over the study period, 2001 – 2021. These trends are statistically
 572 significant ($\alpha=0.01$) for 99 percent of the pixels in the Great Basin (Figure 10b). Though the
 573 earlier part of the data record, 2001-2011, showed increasing LSTs (0.1 °C/yr), the latter part of
 574 the record, 2011-2021, showed a sharply greater rate of increase in LST (0.4 °C/yr).

575

576 We also looked at the daytime and nighttime LST separately using the 1-km daily product (not
 577 shown) and 5-km gridded monthly LST product, MOD21C3 (Figure 11), and found an overall
 578 greater rate of warming during the daytime (0.6 ± 0.25 °C/decade) vs nighttime (0.3 ± 0.12
 579 °C/decade in the Great Basin over the study period. Earlier in the record, the rate of LST
 580 increase was greater during the nighttime (Figure 11).

581

582



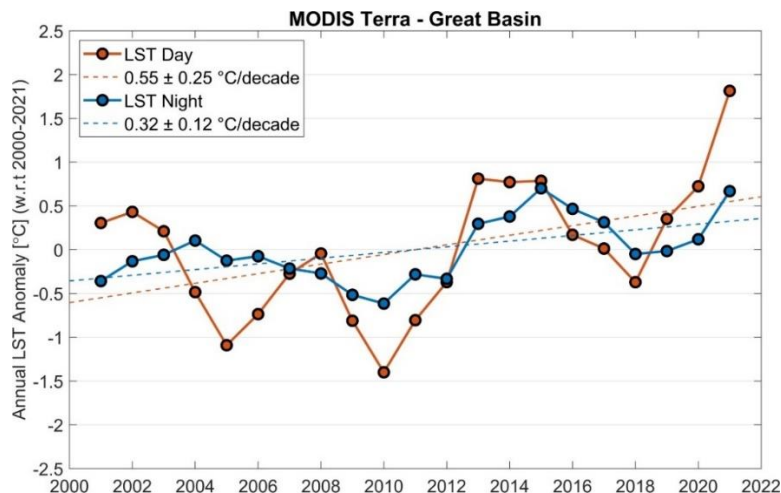
584

585 **Figure 10 a & b.** a) Change in mean LST (average of daytime and nighttime LST) on a per-pixel
 basis. b) Statistically-significant ($\alpha=0.01$) trends in mean LST. There were no statistically-

586 significant trends showing decreasing LSTs in the Great Basin. A water mask shows large lakes
 587 and reservoirs both inside and outside the study domain.

588

589



590

591

592 Figure 11. Annual average land-surface temperature (LST) anomaly (2000 - 2021) for daytime
 593 (red) and nighttime (blue) for the Great Basin, derived from the monthly climate modeling grid
 594 LST product, MOD21C3 (~5-km resolution).

595

596

597 **4.3.1. Changes in LST in the basins of Lake Abert, Great Salt Lake and Mono Lake.** We also
 598 calculated trends in LST and total change in LST using the MOD21A1D and MOD21A1N
 599 products for each lake basin: Lake Abert, GSL and Mono Lake. In all three basins there was an
 600 overall increase in LST, both in the basins and in the lakes, with the greatest total mean change
 601 found in Mono Basin (2.9°C) (Tables 3 & 4). In all three basins, the daytime LST increased
 602 more than did the nighttime LSTs (Table 3). All of the trends are statistically significant
 603 ($\alpha=0.01$). There were no trends of decreasing LST.

604

605

606 **Table 3.** LST increases in °C in the three lake basins, and, in parentheses, rate of increase per
 607 decade, WY 2001 - 2021.

	Lake Abert	Great Salt Lake	Mono Lake
Daytime °C (°C/dec)	3.4 (1.6)	3.1 (1.5)	3.9 (1.9)
Nighttime °C (°C/dec)	1.8 (0.8)	1.7 (0.8)	2.0 (0.9)
Mean °C (°C/dec)	2.6 (1.2)	2.4 (1.2)	2.9 (1.4)

608

609

610 The lake surface-water temperatures also increased (Table 4). Though increases in LST were
 611 measured in Lake Abert, the lake dried up or nearly dried up in 2014, 2015 and 2021, thus the
 612 calculation of trends was not meaningful and the LST increase for Lake Abert is not shown.

613

614

615 **Table 4.** LST increases in °C showing surface-water temperatures of GSL and Mono Lake,
 616 2001 - 2021. Rates of increase per decade are shown in parentheses.

	Great Salt Lake	Mono Lake
Daytime (°C/dec)	1.4 (0.7)	1.8 (0.8)
Nighttime (°C/dec)	0.8 (0.4)	1.2 (0.6)
Mean (°C/dec)	1.1 (0.5)	1.5 (0.7)

617

618

619

620 **4.3.2. Trends in air temperature.** Air temperatures from 164 NOAA meteorological stations
 621 were also analyzed as described in the Methodology section. There is a total increase in mean air
 622 temperature for the Great Basin of ~1.0°C over the 21-year study period, with a slight decrease
 623 in temperature in the first half of the study period and a strong increase during the second half
 624 (Table 5). However, the stations are not evenly spaced throughout the Great Basin, so these
 625 values are not a true mean daily temperature of the Great Basin (see station locations in Figure
 626 5).

627

628

629 **Table 5.** Change in in the Great Basin ‘mean’ air temperatures (°C) in the first half of the study
 630 period, 2001 – 2011, in the second half of the study period, 2011 – 2021, and for the entire study

631 period, 2001 – 2021. (The year 2011 is used in both the first and second halves of the study
632 period.)

Time period	Rate of change (°C/yr)	Total Change (°C)
2001-2011	0	-0.2
2011-2021	0.1	0.9
2001-2021	0.1	1.0

633

634

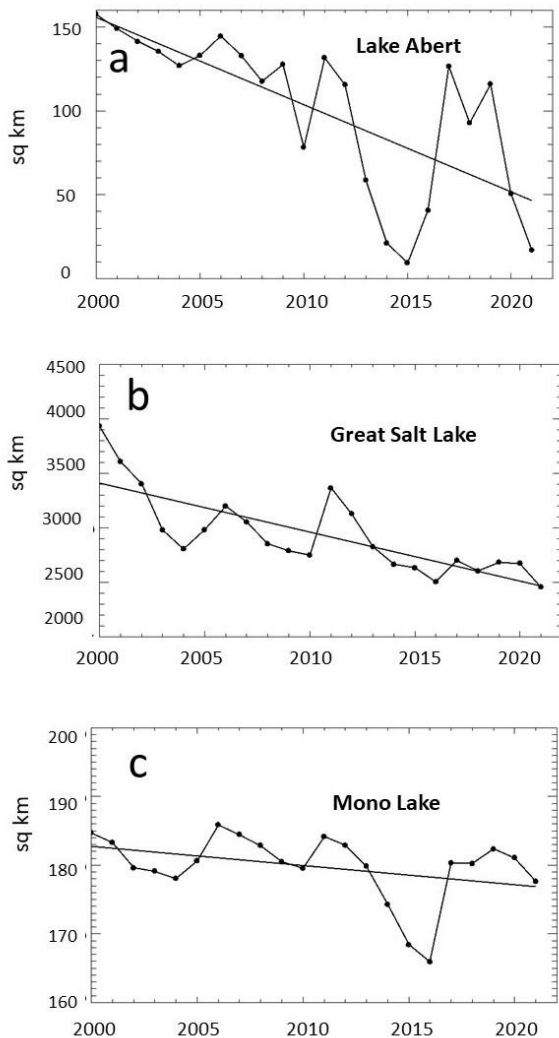
635 **4.3.3. Lake surface-water elevation and extent changes, 2001 – 2021.** Lake Abert has
636 experienced a strong trend toward declining elevation and increasing salinity (Figure 2). The
637 lake elevation has dropped >3.0 m since 2001 when the elevation was 1297.5 m; it was 1293.6 m
638 in 2021, and the lake was essentially dry by the summer of 2022, with 99% of the lakebed
639 exposed. Changes in the areal extent of Lake Abert from 2000 - 2021 are shown in Figure 12a.
640 Discharge from springs along the eastern side has kept the lake from completely desiccating in
641 2022 by maintaining a very shallow pool of water ~1-2 km² in area according to field
642 measurements by one of the authors (RL).

643

644 The GSL surface-water elevation dropped ~1.84 m from 2001 – 2021 (USGS, 2022a). On 23
645 July 2021 the mean surface-water elevation dropped to its lowest recorded level: 1277.5 m, and
646 then continued to drop further (USGS, 2022a). Changes in the areal extent of GSL from 2000 -
647 2021 are shown in Figure 12b.

648

649



650
 651 **Figure 12 a, b & c.** Changes in the areal extents of a) Lake Abert, b) Great Salt Lake and c)
 652 Mono Lake from 2000 through 2021. Lake Abert and Mono Lake extent measurements were
 653 derived from the USGS Dynamic Surface Water Extent product as described in the Methodology
 654 section (USGS, 2022b). The GSL measurements were made using Landsat-7 Enhanced
 655 Thematic Mapper Plus and Landsat-8 OLI imagery and extended from Figure 10a in Hall et al.
 656 (2021).

657
 658
 659 The lake elevation of Mono Lake dropped ~ 0.80 m during the study period (Figure 4) (MLC,
 660 2022a). The areal extent of the lake shrank as well, as compared to length and width

661 measurements acquired in the 1960s (Mason, 1966) (Table 6). Changes in the areal extent of
 662 Mono Lake from 2000 - 2021 are shown in Figure 12c.

663
 664

665 **Table 6.** Length and width measurements of Mono Lake as measured by Mason (1966) and
 666 using Landsat-7 (2001) and Landsat-9 (2022) data products as described in Section 3.2.

667

Date of measurement	Length	Width
Early-to-mid 1960s*	21.76 km	15.34 km
30 July 2001	20.97 km	13.59 km
24 July 2022	20.52 km	13.23 km

668 *An exact date of the measurements was not provided by Mason (1966).

669
 670

671 5. Discussion

672

673 *Drought/climate aridity and reduced snow cover.* The Great Basin is experiencing a more than
 674 two-decades-long drought that began in 1999 - 2000 (Williams et al., 2020). A number of recent
 675 studies have documented an intensifying climate aridity trend across the southwest US (e.g.
 676 Overpeck and Udall, 2020, Woodhouse et al., 2010 and Lian et al., 2021). Since the aridity trend
 677 has been documented in prior studies, our paper focuses on other climate sensitive indicators
 678 available from the MODIS ESDRs and regional station networks, and documents regional
 679 environmental trends interpreted in the context of the increasing aridity trend.

680

681 The trends reported in our study are consistent with a warmer and generally drier climate,
 682 including increasing LST, reduced snow cover, shrinking lakes, and shifting ET patterns.
 683 From 2001 through 2021, we found a mean LST increase of $\sim 2.1^{\circ}\text{C}$ ($\alpha=0.01$) and a mean air
 684 temperature increase of $\sim 1.0^{\circ}\text{C}$ in the Great Basin. The *rate* of increase of both air and surface
 685 temperature has increased since ~ 2011 . If temperatures continue to increase as predicted, the
 686 outcome will be further reductions in regional snow cover, river flows and lake levels,

687 contributing to further increases in atmospheric and soil aridity (Berghuijs et al., 2014; Milly and
688 Dunne, 2020). Regional climate warming is also contributing to drier soil, forest mortality and
689 wildfires (Udall and Overpeck, 2017; Overpeck and Udall, 2020). Part of the reduction in river
690 flows is due to less snow vs rain and thus a reduction in snowmelt reaching streams (see Gordon
691 et al., 2022; Stigter et al., 2018) and perhaps greater evaporative losses from ground previously
692 covered by snow (Milly and Dunne, 2020).

693
694 Greater climate aridity may also be enhancing snowpack sublimation and associated SWE losses
695 to a warmer/drier atmosphere, although total sublimation losses may be offset by reductions in
696 snow-covered area and duration of snow cover (Sexstone et al. 2018). In a dry area such as the
697 Great Basin, sublimation is an especially important factor in the disappearance of snow as
698 atmospheric aridity increases.

699
700 Persistent snow cover in the Great Basin has declined by an average of ~18.4 days over the study
701 period. Approximately 96.1 percent of the area of persistent snow cover (Figure 6a) experienced
702 a reduction in #days of snow cover. However, in the Great Basin and in a larger area of the
703 western US, change in #days of snow cover is generally not statistically significant ($\alpha=0.05$)
704 (Figure S2). An exception is in north-central California and in the Sierra Nevada Mountains
705 where there are clusters of statistically-significant ($\alpha=0.05$) pixels showing declines in #days of
706 snow cover (Figure S2a&b).

707
708 *Mixed trends in evapotranspiration (ET).* We found a positive trend in ET (+3.1 mm total
709 increase) overall for the Great Basin, though there were very few pixels showing statistical
710 significance (Figure 9a & b). In the most sparsely vegetated areas of the Great Basin, such as in
711 most of the lower elevation areas of central and southern Nevada, ET has a larger proportional
712 contribution from soil evaporation (Brust et al., 2021). However, the prolonged drought has
713 extended the period of exceptionally dry soil conditions, reducing evaporation accordingly. This
714 has contributed to overall reduction in ET in the drought-affected areas. This is a reinforcing
715 feedback: lower ET results in a drier atmosphere (larger vapor pressure deficit and higher LST),
716 with further ET reductions (Lian et al., 2021). The large areas of neutral and even decreasing
717 trends in ET are consistent with the expected ET reduction from the extended drought in the

718 Great Basin. The lack of ET increase over much of the Great Basin may contribute to higher
719 LST since more net radiant energy is partitioned as sensible rather than latent heat, which would
720 reinforce warming. Declining ET in parts of the Great Basin and in California contrast with ET
721 increases seen elsewhere in the western US where there are large areas of statistically-significant
722 ($\alpha=0.05$) increases in ET (Figure S3).

723
724 Positive, statistically significant ($\alpha=0.05$) ET trends are seen along the mountainous edges of the
725 eastern Great Basin in the higher elevations of the Wasatch Mountains and the Colorado Plateau
726 (Figures 1 and 9a&b). These areas have a cooler/wetter climate and greater vegetation cover
727 compared to lower elevation areas in the Great Basin. The generally greater moisture availability
728 and increasingly earlier snowmelt may contribute to higher ET rates, especially in spring and
729 early summer. Positive ET trends, particularly in the northern parts of the basin, also coincide
730 with a small increase in irrigated cropland (Ketchum et al. 2020) which can elevate ET by
731 enhancing cropland vegetation growth and reducing surface evaporative resistance relative to the
732 surrounding natural semi-arid vegetation.

733
734 Over the study period, ET in the GSL Basin increased an average of ~28.1 mm. There may also
735 be a secondary precipitation/temperature/snow/elevation effect on the ET trend in the GSL basin,
736 where the higher elevation areas can maintain positive ET trends as the climate warms due to the
737 more moderate temperatures and generally higher annual precipitation amounts, along with
738 additional spring moisture inputs from seasonal snowmelt that can sustain ET.

739
740 *Response of lakes to increasing temperatures and reduced snow cover.* Warmer temperatures
741 and associated greater atmospheric moisture demand are likely driving increasing rates of
742 evaporation of water in lakes, since evaporation over a lake surface is largely unrestricted in
743 summer ((see interactive database of 1.42 million lakes worldwide (Zhao et al., 2022)). Positive
744 trends in lake evaporation due to higher water surface temperatures are likely contributing to
745 desiccation. We measured increasing surface water temperature on GSL and Mono Lake (Table
746 4). Schneider et al. (2009) reported that Mono Lake experienced a summer nighttime surface-
747 water temperature warming of $0.2\pm 0.02^\circ\text{C}/\text{yr}$, 1992 – 2009, for a total increase of 2.6°C , over the
748 17-year study period. This may be compared with the LST warming that we measured on Mono

749 Lake (1.5°C), though for a different time period, but overlapping with the Schneider et al. (2009)
750 study period.

751

752 Additionally, as a snowpack declines in mountainous areas, higher air temperatures will warm
753 the lake-surface water faster when less snowmelt flows into the lakes (Smits et al., 2020). The
754 decline in seasonal snow cover is also likely contributing to LST warming at the higher
755 elevations in the Great Basin.

756

757 *Deleterious effects on wildlife and humans.* Lake desiccation can be life threatening to humans
758 and wildlife. Expansion of dry lakebeds allows toxic dust and particulate matter to be picked up
759 by wind and become airborne, creating air pollution that includes heavy metals. Owens Lake, on
760 the eastern side of the Sierra Nevada Mountains in California, became desiccated after the City
761 of Los Angeles diverted inflow from the Owens River, which leads to the lake, to augment the
762 city's water supply. Before that diversion project began in 1913, the lake covered an area of ~
763 280 km² (Reheis, 2022); now it is mostly dry. 'Saline dust' from the dried lake basin is a major
764 source of PM10 dust pollution and has adversely affected vegetation and soils surrounding the
765 lake (Zucca et al., 2021). The City of Los Angeles will spend billions of dollars over 25 years to
766 minimize airborne "dust" from the Owens Lake basin (Robinson, 2018).

767

768 Residents living near Mono Lake in California and Great Salt Lake in Utah are also at risk for
769 hazardous air quality due to the expanding lakebeds (Stine, 1991; Reynolds et al., 2014; MLC,
770 2022a). The population exceeds 2 million people in Salt Lake City and other rapidly-growing
771 cities along the Wasatch Front, which are affected by the expansion of the shoreline of GSL
772 (Putman et al., 2022). Furthermore, when the dust is deposited in the nearby snow-covered
773 Wasatch and Uinta mountains to the east of GSL, it reduces the albedo of the snow surface
774 allowing greater absorption of solar radiation that accelerates snowmelt (Skiles et al., 2018).

775

776 If the drought continues and perhaps even intensifies, water demand for irrigation and for urban
777 areas will increase, thus there will be even less water available to flow into the lakes. In
778 response to the increased aridity, water supplies may be increased by allowing more groundwater
779 use and funding the construction of reservoirs, both of which would negatively affect

780 downstream natural lakes. The need for water to flow into the Great Basin lakes should,
781 however, be considered in order to avert environmental and economic catastrophes, such as
782 occurred with the desiccation of Owens Lake, California.

783
784 *Changes in lake area and depth.* While the changes in areal extent of Lake Abert and Great Salt
785 Lake are dramatic (see Section 4.3.3), changes in the extent of Mono Lake are not as great
786 because of its greater depth, together with legal actions enacted to slow its decline. Mono Lake
787 is much deeper than the other two lakes and its shape does not lend itself to large changes in
788 areal extent with small decreases in volume. However, at the end of the 2021 WY, the surface-
789 water elevation of Mono Lake was 3.3 m lower than the surface-water elevation target of ~1948
790 m which would cover much of the exposed dry lakebed and allow a healthy ecosystem to thrive
791 and protect wildlife habitat (MLC, 2022a).

792
793 The small spring-fed pool present in 2021 and 2022 in the lakebed of Lake Abert provided some
794 habitat for 5-10 thousand migratory waterbirds, but this was just a fraction of the hundreds of
795 thousands of birds that use the lake (Larson et al., 2016) when water levels are higher.

796

797

798 6. Conclusion

799

800 Analysis of more than two decades of data from satellite-derived ESDRs developed from
801 validated NASA standard data products (snow cover, LST and ET) from the Terra MODIS
802 sensor, along with ancillary data, has enabled an in-depth evaluation of some of the
803 environmental effects of the megadrought on terminal lakes in the Great Basin. Higher air and
804 surface temperatures and a reduction in the #days of snow cover and lower SWE promote
805 desiccation of terminal lakes, endangering human health, wildlife habitat, and incurring dire
806 economic consequences.

807

808 The basins of Lake Abert, Oregon, Great Salt Lake, Utah and Mono Lake, California, located in
809 different areas and different topographical and climate zones within the Great Basin, are

810 responding differently to intensifying warming and aridification. Though all show 21-year
811 trends toward increasing temperatures and decreasing #days of snow cover, the ET results are
812 mixed. The MODIS ESDRs used in this study only cover a 21-year period, although continuing
813 satellite operations are approaching the 30-year threshold for defining Climate Normals, and may
814 enable greater precision in documenting climate trends.

815
816 Over the 2001-2021 study period, the Great Basin experienced a $\sim 1.0^{\circ}\text{C}$ increase in air
817 temperature and a 2.1°C increase in LST, with a greater rate of increase in the latter half of the
818 study period for both LST and air temperature. Mono Basin shows a slightly greater LST
819 increase (2.9°C) than the Lake Abert (2.6°C) and GSL (2.4°C) basins. There appears to be a
820 breakpoint around 2011 when the rate of warming in both LST and air temperature increases, for
821 reasons that are unclear. A loss of #days of persistent snow cover is seen in the Great Basin (-
822 18.4 days average) and in the individual lake basins. Mono Basin shows the greatest loss, for a
823 total of ~ 28.4 days, with the basins of Lake Abert and GSL showing more modest losses for a
824 total of 14.6 days and 14.1 fewer #days of persistent snow cover, respectively. In general, the
825 GSL and Mono basins show positive ET trends, while Lake Abert shows slightly negative ET
826 trends associated with increasingly sparse vegetation and warm, dry conditions. The overall
827 change in ET for the Great Basin is positive (3.1 mm), but relatively small due to heterogeneity
828 in the sign and magnitude of the regional trends.

829
830 Lake Abert, the shallowest of the three study lakes, was almost fully desiccated in 2021 while
831 GSL reached its lowest surface-water elevation ever recorded in 2021 and has declined further
832 since then. Legislation prompted a slowing in the rate of decline of Mono Lake, but despite this
833 it has continued to decline, and is ~ 3.3 m lower than its mandated elevation.

834
835 If the climate in the US West continues to get warmer and drier, as predicted, the societal
836 demand for water will also continue to increase. The example of Owens Lake, California, shows
837 that the diversion of stream water from saline lakes comes at a huge cost to human health
838 especially when a terminal lake is near a population center. Costly mitigation efforts are
839 necessitated, though only after widespread adverse health impacts have been identified.
840 Controlling upstream water diversions may help to alleviate severe and costly ecological and

841 human health consequences associated with continued desiccation of terminal lakes in the Great
842 Basin and elsewhere.

843

844

845 Acknowledgements

846 We thank Dr. K. Arthur Endsley, Numerical Terradynamic Simulation Group, University of
847 Montana, for his review of the MOD16A2GF evapotranspiration product results. This work was
848 supported by NASA's Terrestrial Hydrology Program and Earth Observing Systems programs:
849 80NSSC22K0554, 80NSSC21K1927 and WBS number: 444491.02.01.04.52. The authors
850 declare no real or perceived financial conflicts of interest.

851

852

853 Data Availability Statement

854 All of the data used to undertake this research are freely available. The specific sources for the
855 data are provided in the text and summarized below.

856 MODIS snow-cover [Dataset]: <https://modis-snow-ice.gsfc.nasa.gov/?c=MOD10A1F>

857 MODIS LST [Dataset]: <https://lpdaac.usgs.gov/products/mod21a1dv061/> and

858 <https://lpdaac.usgs.gov/products/mod21a1nv061/>

859 MODIS ET [Dataset]: <https://lpdaac.usgs.gov/products/mod16a2v006/>

860 Air temperature: NOAA NCEI [Dataset]: <https://www.ncei.noaa.gov/maps/daily-summaries/>

861 SNODAS [Dataset]: NOAA NOHRSC: <https://nsidc.org/data/g02158/versions/1>

862 SNOTEL [Dataset]: USDA NRCS:

863 <https://wcc.sc.egov.usda.gov/nwcc/rgrpt?report=precsnotelmon&state=CA>

864 <https://wcc.sc.egov.usda.gov/nwcc/rgrpt?report=precsnotelmon&state=OR&operation=View>

865 <https://wcc.sc.egov.usda.gov/nwcc/rgrpt?report=precsnotelmon&state=UT>

866

867

868

References

869

870 Audubon, 2022: National Audubon Society, Great Salt Lake,
871 <https://www.audubon.org/conservation/project/great-salt-lake> , last accessed 8/11/2022

872

873 Bajgain, R., Xiao, X., Wagle, P., Kimball, J. S., Brust, C., Basara, J. B., ... & Neel, J. P. (2020).
874 Comparing evapotranspiration products of different temporal and spatial scales in native and
875 managed prairie pastures. *Remote Sensing*, 13(1), 82. <https://doi.org/10.3390/rs13010082>

876

877 Berghuijs, W. R., Woods, R. A., & Hrachowitz, M. (2014). A precipitation shift from snow
878 towards rain leads to a decrease in streamflow. *Nature climate change*, 4(7), 583-586.

879

880 Brust, C., Kimball, J. S., Maneta, M. P., Jencso, K., He, M., & Reichle, R. H. (2021). Using
881 SMAP Level-4 soil moisture to constrain MOD16 evapotranspiration over the contiguous USA.
882 *Remote Sensing of Environment*, 255, 112277.

883

884 CEOS-LPV, 2022: Committee on Earth Observation Satellites - Land Product Validation
885 subgroup, <https://lpvs.gsfc.nasa.gov/>, last accessed 8/7/2022.

886

887 Carroll, T., Cline, D., Fall, G., Nilsson, A., Li, L. & Rost, A., 2001. NOHRSC Operations and
888 the Simulation of Snow Cover Properties for the Conterminous U.S. *Proceedings of the 69th*
889 *Annual Meeting of the Western Snow Conference*, pp. 1-14.

890

891 Conte, F. P., Jellison, R. S., & Starrett, G. L. (1988). Nearshore and pelagic abundances of
892 *Artemia monica* in Mono Lake, California. *Hydrobiologia*, 158(1), 173-181.

893

894 Cook, E. R., Woodhouse, C. A., Eakin, C. M., Meko, D. M., & Stahle, D. W. (2004). Long-term
895 aridity changes in the western United States. *Science*, 306(5698), 1015-1018

896 <https://doi:10.1126/science.1102586>

897
898 Cook, B. I., Ault, T. R., & Smerdon, J. E. (2015). Unprecedented 21st century drought risk in the
899 American Southwest and Central Plains. *Science Advances*, *1*(1), e1400082.
900
901 Dannenberg, M. P., Yan, D., Barnes, M. L., Smith, W. K., Johnston, M. R., Scott, R. L., ...
902 (2022). Exceptional heat and atmospheric dryness amplified losses of primary production during
903 the 2020 US Southwest hot drought. *Global Change Biology*. <https://doi.org/10.1111/gcb.16214>
904
905 Derouin, S., 2017: Utah's Great Salt Lake has lost half of its water, thanks to thirsty humans.
906 *Science*. [https://www.sciencemag.org/news/2017/11/utah-s-great-salt-lake-has-lost-half-its-](https://www.sciencemag.org/news/2017/11/utah-s-great-salt-lake-has-lost-half-its-water-thanks-thirsty-humans)
907 [water-thanks-thirsty-humans](https://www.sciencemag.org/news/2017/11/utah-s-great-salt-lake-has-lost-half-its-water-thanks-thirsty-humans)
908
909 Déry, S. J., & Brown, R. D. (2007). Recent Northern Hemisphere snow cover extent trends and
910 implications for the snow-albedo feedback. *Geophysical Research Letters*, *34*(22).
911 <https://doi:10.1029/2007/GL031474>
912
913 Donnelly, J. P., King, S. L., Silverman, N. L., Collins, D. P., Carrera-Gonzalez, E. M., Lafón-
914 Terrazas, A., & Moore, J. N. (2020). Climate and human water use diminish wetland networks
915 supporting continental waterbird migration. *Global Change Biology*, *26*(4), 2042-2059.
916
917 Ficklin, D. L., & Novick, K. A. (2017). Historic and projected changes in vapor pressure deficit
918 suggest a continental-scale drying of the United States atmosphere. *Journal of Geophysical*
919 *Research: Atmospheres*, *122*(4), 2061-2079. <https://doi:10.1002/2016JD025855>.
920
921 Ficklin, D. L., Stewart, I. T., & Maurer, E. P. (2013). Effects of projected climate change on the
922 hydrology in the Mono Lake Basin, California. *Climatic Change*, *116*(1), 111-131.
923 <https://doi.org/10.1007/s10584-012-0566-6>
924
925 Frankson, R. and Kunkel, K. (2016) Utah, NOAA NCEI State Summaries 149-UT [Dataset].
926 <https://statesummaries.ncics.org/chapter/ut/> last accessed 8/24/2022
927

- 928 Gordon, B. L., Brooks, P. D., Krogh, S. A. Boisrame, G. F., Carroll, R. W., McNamara, J. P., &
929 Harpold, A. A. (2022). Why does snowmelt-driven streamflow response to warming vary? A
930 data-driven review and predictive framework. *Environmental Research Letters*.
931 <https://doi.org/10.1088/1748-9326/ac64b4>.
- 932
- 933 Haig, S. M., Murphy, S. P., Matthews, J. H., Arismendi, I., & Safeeq, M. (2019). Climate-altered
934 wetlands challenge waterbird use and migratory connectivity in arid landscapes. *Scientific*
935 *Reports*, 9(1), 1-10.
- 936
- 937 Hall, D. K., Riggs, G. A., Foster, J. L., & Kumar, S. V. (2010). Development and evaluation of a
938 cloud-gap-filled MODIS daily snow-cover product. *Remote Sensing of Environment*, 114(3),
939 496-503. <https://doi.org/10.1016/j.rse.2009.10.007>
- 940
- 941 Hall, D. K., Riggs, G. A., DiGirolamo, N. E., & Román, M. O. (2019). Evaluation of MODIS
942 and VIIRS cloud-gap-filled snow-cover products for production of an Earth science data record.
943 *Hydrology and Earth System Sciences*, 23(12), 5227-5241.
944 <https://doi.org/10.5194/hess-23-5227-2019>
- 945
- 946 Hall, D. K. and G. A. Riggs. 2020. *MODIS/Terra CGF Snow Cover Daily L3 Global 500m SIN*
947 *Grid, Version 61* [Dataset]. Boulder, Colorado USA. NASA National Snow and Ice Data Center
948 Distributed Active Archive Center. <https://doi.org/10.5067/MODIS/MOD10A1F.061>. [Accessed
949 7/9/2022].
- 950
- 951 Hall, D. K., O'Leary III, D. S., DiGirolamo, N. E., Miller, W., & Kang, D. H. (2021). The role of
952 declining snow cover in the desiccation of the Great Salt Lake, Utah, using MODIS data. *Remote*
953 *Sensing of Environment*, 252, 112106. <https://doi.org/10.1016/j.rse.2020.112106>
- 954
- 955 Herbst, D.B., 2014: Mono Lake: stream taken and given back, but still waiting, *LakeLine*, fall
956 2014, 21 – 24.
- 957

- 958 Hulley, G., Hook, S. (2021a). MODIS/Terra Land Surface Temperature/3-Band Emissivity Daily
959 L3 Global 1km SIN Grid Day V061 [Dataset]. NASA EOSDIS Land Processes DAAC.
960 Accessed 07/09/2022 from <https://doi.org/10.5067/MODIS/MOD21A1D.061>
961
- 962 Hulley, G., Hook, S. (2021b). MODIS/Terra Land Surface Temperature/3-Band Emissivity Daily
963 L3 Global 1km SIN Grid Night V061 [Dataset]. NASA EOSDIS Land Processes DAAC.
964 Accessed 07/09/2022 from <https://doi.org/10.5067/MODIS/MOD21A1N.061>
965
- 966 Hulley, G. C., Malakar, N., Islam, T., Freepartner, R. (2017). NASA's MODIS and VIIRS Land
967 Surface Temperature and Emissivity Products: A Consistent and High Quality Earth System
968 Data Record. *IEEE Trans. Geosci. and Remote Sensing*, 11(2), 522-535.
969 <https://doi.org/10.1109/JSTARS.2017.2779330>.
970
- 971 Jones, J.W. (2019). Improved Automated Detection of Subpixel-Scale Inundation—Revised
972 Dynamic Surface Water Extent (DSWE) Partial Surface Water Tests. *Remote Sens.*, 11,
973 374, <https://doi.org/10.3390/rs11040374>.
974
- 975 Ketchum, D., Jencso, K., Maneta, M. P., Melton, F., Jones, M. O., & Huntington, J. (2020).
976 IrrMapper: A machine learning approach for high resolution mapping of irrigated agriculture
977 across the Western US. *Remote Sensing*, 12(14), 2328. <https://doi.org/10.3390/rs12142328>
978
- 979 Kumar, S., Mocko, D., Vuyovich, C., & Peters-Lidard, C. (2020). Impact of surface albedo
980 assimilation on snow estimation. *Remote Sensing*, 12(4), 645.
981 <https://doi.org/10.3390/rs12040645>
982
- 983 LDOPE, 2022: Land Data Operational Product Evaluation, What is Data Outage?
984 https://landweb.modaps.eosdis.nasa.gov/cgi-bin/QS/new/pages.cgi?name=data_outage last
985 accessed 8/12/2022.
986
- 987 Larson, D. and R. Larson, 2011: Lake Abert, OR, LakeLine, winter 2011, 47-58.
988

- 989 Larson, R. and Eilers, J., 2014. Lake Abert, OR: a terminal lake under extreme water stress.
990 LakeLine, 34, 30-33.
991
- 992 Larson, R., Eilers, J., Kreuz, K., Pecher, W. T., DasSarma, S., & Dougill, S. (2016). Recent
993 desiccation-related ecosystem changes at Lake Abert, Oregon: a terminal alkaline salt lake.
994 *Western North American Naturalist*, 76(4), 389-404.
995 <https://doi.org/10.3398/064.076.0402>
996
- 997 Lian, X., Piao, S., Chen, A., Huntingford, C., Fu, B., Li, L. Z., ... & Roderick, M. L. (2021).
998 Multifaceted characteristics of dryland aridity changes in a warming world. *Nature Reviews*
999 *Earth & Environment*, 2(4), 232-250.
1000
- 1001 MBC (2022) Mono Basin Clearinghouse,
1002 <http://www.monobasinresearch.org/data/levelmonthly.php> - last accessed 8/17/2022.
1003
- 1004 MLC (2022a). Mono Lake Committee, Another drought year for Mono Lake,
1005 <https://www.monolake.org/today/another-drought-year-for-mono-lake/>, last accessed 8/11/2022.
1006
- 1007 MLC (2022b). State of the Lake, <https://www.monolake.org/learn/stateofthelake/> and Birds,
1008 <https://www.monolake.org/about/ecobirds> last accessed 8/6/2022.
1009
- 1010 McCabe, G.J., Wolock, D.M. (2010). Long-term variability in Northern Hemisphere snow cover
1011 and associations with warmer winters. *Climatic Change* **99**, 141–153.
1012 <https://doi.org/10.1007/s10584-009-9675-2>
1013
- 1014 McKenzie, D., & Littell, J. S. (2017). Climate change and the eco-hydrology of fire: Will area
1015 burned increase in a warming western USA? *Ecological Applications*, 27(1), 26-36.
1016 <https://doi.org/10.1002/eap.1420>
1017

- 1018 Mason, D.T. (1966). Limnology of Mono Lake, California, University of California Publication
1019 66-13-145, Ph.D. Dissertation, Zoology, Univ. of California – Davis, 83, 110p, University
1020 Microfilms, Inc., Ann Arbor, MI.
1021
- 1022 Melack, J. M. (1983). Large, deep salt lakes: a comparative limnological analysis.
1023 *Hydrobiologia*, 105(1), 223-230.
1024
- 1025 Milly, P. C., & Dunne, K. A. (2020). Colorado River flow dwindles as warming-driven loss of
1026 reflective snow energizes evaporation. *Science*, 367(6483), 1252-1255.
1027 <https://doi:10.1126/science.aay9187>
1028
- 1029 Mu, Q., Zhao, M., & Running, S. W. (2011). Improvements to a MODIS global terrestrial
1030 evapotranspiration algorithm. *Remote Sensing of Environment*, 115(8), 1781-1800.
1031
- 1032 NCEI (2022) NOAA National Centers for Environmental Information, Daily Summaries Version
1033 3.1.0, Global Historical Climate Network includes daily land surface observations from around
1034 the world [Dataset]. [<https://www.ncei.noaa.gov/maps/daily-summaries/>] - last accessed
1035 7/28/2022].
1036
- 1037 NOHRSC, 2004. National Operational Hydrologic Remote Sensing Center, *Snow Data*
1038 *Assimilation System (SNODAS) Data Products at NSIDC, Version 1* [Dataset]. Boulder,
1039 Colorado USA. NSIDC: National Snow and Ice Data Center,
1040 <https://nsidc.org/data/g02158/versions/1>, last accessed 8/14/2022.
1041
- 1042 NRC 1987. *The Mono Basin Ecosystem: Effects of Changing Lake Level*, Washington, DC: The
1043 National Academies Press. <https://doi.org/10.17226/1007>
1044
- 1045 NRCS, 2022: National Resources Conservation Service,
1046 <https://wcc.sc.egov.usda.gov/nwcc/rgrpt?report=precspotelmon&state=CA> (for California);
1047 <https://wcc.sc.egov.usda.gov/nwcc/rgrpt?report=precspotelmon&state=OR&operation=View> (for

- 1048 Oregon), <https://wcc.sc.egov.usda.gov/nwcc/rgprpt?report=precspotelmon&state=UT> (for Utah),
1049 Last accessed 8/13/2022.
1050
- 1051 Nielsen, L. C., & DePaolo, D. J. (2013). Ca isotope fractionation in a high-alkalinity lake
1052 system: Mono Lake, California. *Geochimica et Cosmochimica Acta*, 118, 276-294.
1053 <https://doi.org/10.1016/j.gca.2013.05.007> .
1054
- 1055 O'Reilly, C. M., Sharma, S., Gray, D. K., Hampton, S. E., Read, J. S., Rowley, R. J. ... (2015).
1056 Rapid and highly variable warming of lake surface waters around the globe. *Geophysical*
1057 *Research Letters*, 42(24), 10-773. <https://doi.org/10.1002/2015GL066235>
1058
- 1059 Oring, L. W., & Reed, J. M. (1997). Shorebirds of the western Great Basin of North America:
1060 overview and importance to continental populations. *International Wader Studies*, 9, 6-12.
1061
- 1062 Overpeck, J. T., & Udall, B. (2020). Climate change and the aridification of North America.
1063 *Proceedings of the National Academy of Sciences*, 117(22), 11856-11858.
1064
- 1065 Phillips, K. N., & Van Denburgh, A. S. (1971). *Hydrology and geochemistry of Abert, Summer,*
1066 *and Goose Lakes and other closed-basin lakes in south-central Oregon*. US Government
1067 Printing Office.
1068
- 1069 Piechota, T., Timilsena, J., Tootle, G., & Hidalgo, H. (2004). The western US drought: How bad
1070 is it? *Eos, Transactions American Geophysical Union*, 85(32), 301-304.
1071 <https://doi.org/10.1029/2004EO320001>
1072
- 1073 Putman, A. L., Jones, D. K., Blakowski, M. A., DiViesti, D., Hynek, S. A., Fernandez, D. P. &
1074 Mendoza, D. (2022). Industrial particulate pollution and historical land use contribute metals of
1075 concern to dust deposited in neighborhoods along the Wasatch Front, UT, USA. *GeoHealth*, 6,
1076 e2022GH000671. <https://doi.org/10.1029/2022GH000671>
1077

- 1078 Reheis, M.C. (2022) Owens (Dry) Lake, California: A human-induced dust problem, USGS,
1079 <https://geochange.er.usgs.gov/sw/impacts/geology/owens/>
1080
- 1081 Reynolds, R. L., Goldstein, H. L., Moskowitz, B. M., Bryant, A. C., Skiles, S. M., Kokaly, R. F.
1082 ... (2014). Composition of dust deposited to snow cover in the Wasatch Range (Utah, USA):
1083 Controls on radiative properties of snow cover and comparison to some dust-source sediments.
1084 *Aeolian Research*, 15, 73-90.
1085
- 1086 Riggs, G. A., Hall, D. K., & Román, M.O. (2018). MODIS snow products user guide for
1087 Collection 6.1 (C6.1). Available at: <https://modis-snow-ice.gsfc.nasa.gov/?c=userguides> last
1088 accessed 3/17/2019.
1089
- 1090 Riggs, G., & Hall, D. (2020). Continuity of MODIS and VIIRS snow cover extent data products
1091 for development of an Earth science data record. *Remote Sensing*, 12(22), 3781.
1092
- 1093 Roberts, M. F. (2005). Organic compatible solutes of halotolerant and halophilic
1094 microorganisms. *Saline Systems*, 1(1), 1-30.
1095
- 1096 Robinson, A., & Davis, B. (2018). From solution space to interface: Six actions for landscape
1097 infrastructure design. In *Codify* (pp. 155-168). Routledge.
1098
- 1099 Romero, J. R., & Melack, J. M. (1996). Sensitivity of vertical mixing in a large saline lake to
1100 variations in runoff. *Limnology and Oceanography*, 41(5), 955-965.
1101 <https://doi.org/10.4319/lo.1996.41.5.0955>
1102
- 1103 Running, S., Mu, Q., Zhao, M., Moreno, A. (2021). MODIS/Terra Net Evapotranspiration Gap-
1104 Filled 8-Day L4 Global 500m SIN Grid V061 [Dataset]. NASA EOSDIS Land Processes
1105 DAAC. Accessed 2022-07-09 from <https://doi.org/10.5067/MODIS/MOD16A2GF.061>
1106
- 1107 SNODAS, 2022: National Operational Hydrologic Remote Sensing Center. Snow Data
1108 Assimilation System (SNODAS) Data Products at NSIDC, Version 1 [Dataset] 2004, Distributed

1109 by National Snow and Ice Data Center. <https://doi.org/10.7265/N5TB14TC>. Date Accessed 08-
1110 [07-2022](https://doi.org/10.7265/N5TB14TC).
1111
1112 Schneider, P., Hook, S. J., Radocinski, R. G., Corlett, G. K., Hulley, G. C., Schladow, S. G., &
1113 Steissberg, T. E. (2009). Satellite observations indicate rapid warming trend for lakes in
1114 California and Nevada. *Geophysical Research Letters*, 36(22).
1115 <https://doi.org/10.1029/2009GL040846>
1116
1117 Sexstone, G. A., Clow, D. W., Fassnacht, S. R., Liston, G. E., Hiemstra, C. A., Knowles, J. F., &
1118 Penn, C. A. (2018). Snow sublimation in mountain environments and its sensitivity to forest
1119 disturbance and climate warming. *Water Resources Research*, 54(2), 1191-1211.
1120 <https://doi.org/10.1002/2017WR021172>
1121
1122 Senner, N. R., Moore, J. N., Seager, S. T., Dougill, S., Kreuz, K., & Senner, S. E. (2018). A salt
1123 lake under stress: Relationships among birds, water levels, and invertebrates at a Great Basin
1124 saline lake. *Biological Conservation*, 220, 320-329.
1125
1126 Skiles, S. M., Mallia, D. V., Hallar, A. G., Lin, J. C., Lambert, A., Petersen, R., & Clark, S.
1127 (2018). Implications of a shrinking Great Salt Lake for dust on snow deposition in the Wasatch
1128 Mountains, UT, as informed by a source to sink case study from the 13–14 April 2017 dust
1129 event. *Environmental Research Letters*, 13(12), 124031. [https://doi.org/10.1088/1748-
1130 9326/aaefd8](https://doi.org/10.1088/1748-9326/aaefd8)
1131
1132 Smits, A. P., MacIntyre, S., & Sadro, S. (2020). Snowpack determines relative importance of
1133 climate factors driving summer lake warming. *Limnology and Oceanography Letters*, 5(3), 271-
1134 279. <https://doi.org/10.1002/lol2.10147>
1135
1136 Snyder, K. A., Evers, L., Chambers, J. C., Dunham, J., Bradford, J. B., & Loik, M. E. (2019).
1137 Effects of changing climate on the hydrological cycle in cold desert ecosystems of the Great
1138 Basin and Columbia Plateau. *Rangeland Ecology & Management*, 72(1), 1-12.
1139

- 1140 Sorensen, E. D., Hoven, H. M. & Neill, J. (2020). Great Salt Lake shorebirds, their habitats, and
1141 food base. In *Great Salt Lake Biology*, pp. 263-309. Springer, Cham.
1142
- 1143 Stigter, E. E., Litt, M., Steiner, J. F., Bonekamp, P. N., Shea, J. M., Bierkens, M. F., &
1144 Immerzeel, W. W. (2018). The importance of snow sublimation on a Himalayan glacier.
1145 *Frontiers in Earth Science*, 6, 108.
1146
- 1147 Stine, S. (1991). Geomorphic, geographic, and hydrographic basis for resolving the Mono Lake
1148 controversy. *Environmental Geology and Water Sciences*, 17(2), 67-83.
1149 <https://doi.org/10.1007/BF01701564>
1150
- 1151 USGS National Map (2019). [https://www.usgs.gov/programs/national-geospatial-](https://www.usgs.gov/programs/national-geospatial-program/national-map)
1152 [program/national-map](https://www.usgs.gov/programs/national-geospatial-program/national-map) last accessed 8/24/2022
1153
- 1154 USGS GTOPO30 DEM, 2019. [https://www.usgs.gov/centers/eros/science/usgs-eros-archive-](https://www.usgs.gov/centers/eros/science/usgs-eros-archive-digital-elevation-global-30-arc-second-elevation-gtopo30?qt-science_center_objects=0#qt-science_center_objects)
1155 [digital-elevation-global-30-arc-second-elevation-gtopo30?qt-science_center_objects=0#qt-](https://www.usgs.gov/centers/eros/science/usgs-eros-archive-digital-elevation-global-30-arc-second-elevation-gtopo30?qt-science_center_objects=0#qt-science_center_objects)
1156 [science_center_objects](https://www.usgs.gov/centers/eros/science/usgs-eros-archive-digital-elevation-global-30-arc-second-elevation-gtopo30?qt-science_center_objects=0#qt-science_center_objects) last accessed 12/12/2019, <https://doi.org/10.3133/fs20193032>
1157
- 1158 USGS (2020). National Water Information System: Web Interface
1159 <https://waterdata.usgs.gov/nwis/rt> last accessed 8/24/2022, <https://doi.org/10.5066/F7P55KJN>
1160
- 1161 USGS (2022a) USGS National Water Information System
1162 <https://waterdata.usgs.gov/ut/nwis/current?type=lake>, last accessed 8/24/2022,
1163 <https://doi.org/10.5066/F7P55KJN>
1164
- 1165 USGS (2022b) Landsat Collection 2 Level-3 Dynamic Surface Water Extent Science Product
1166 [Dataset]. [https://www.usgs.gov/landsat-missions/landsat-collection-2-level-3-dynamic-surface-](https://www.usgs.gov/landsat-missions/landsat-collection-2-level-3-dynamic-surface-water-extent-science-product)
1167 [water-extent-science-product](https://www.usgs.gov/landsat-missions/landsat-collection-2-level-3-dynamic-surface-water-extent-science-product) .
1168

- 1169 Udall, B., & Overpeck, J. (2017). The twenty-first century Colorado River hot drought and
1170 implications for the future. *Water Resources Research*, 53(3), 2404-2418.
1171 <https://doi.org/10.1002/2016WR019638>
1172
- 1173 Vorster, P. (1985). *A water balance forecast model for Mono Lake, California* (Master's thesis,
1174 Calif. State University, Hayward).
1175
- 1176 White, J. S., Null, S. E., & Tarboton, D. G. (2014a). Modeled changes to Great Salt Lake salinity
1177 from railroad causeway alteration. *Final Report to the Utah Division of Forestry, Fire and State*
1178 *Lands*.
1179
- 1180 White, J.S., S.E. Null & D. Tarboton (2014b). More than meets the eye: Managing salinity in the
1181 Great Salt Lake, Utah, *LakeLine Magazine*, 34(3):25-29. [https://www.nalms.org/nalms-](https://www.nalms.org/nalms-memberships/)
1182 [memberships/](https://www.nalms.org/nalms-memberships/)
1183
- 1184 White, J. S., Null, S. E., & Tarboton, D. G. (2015). How do changes to the railroad causeway in
1185 Utah's Great Salt Lake affect water and salt flow?. *PloS one*, 10(12), e0144111.
1186 <https://doi.org/10.1371/journal.pone.0144111>
1187
- 1188 Williams, A. P., Cook, E. R., Smerdon, J. E., Cook, B. I., Abatzoglou, J. T., Bolles, K., ... &
1189 Livneh, B. (2020). Large contribution from anthropogenic warming to an emerging North
1190 American megadrought. *Science*, 368(6488), 314-318. <https://doi:10.1126/science.aaz9600>
1191
- 1192 Williams, A. P., Cook, B. I., & Smerdon, J. E. (2022). Rapid intensification of the emerging
1193 southwestern North American megadrought in 2020–2021. *Nature Climate Change*, 12(3), 232-
1194 234.
1195
- 1196 Woodhouse, C.A., Meko, D.M., MacDonald, G.M., Stahle, D.W. and Cook, E.R. (2010). A
1197 1,200-year perspective of 21st century drought in southwestern North America. *Proceedings of*
1198 *the National Academy of Sciences*, 107(50):21283-21288.
1199 <https://doi.org/10.1073/pnas.0911197107>

- 1200
- 1201 Wurtsbaugh, W. A., Miller, C., Null, S. E., DeRose, R. J., Wilcock, P., Hahnenberger, M., ...
1202 (2017). Decline of the world's saline lakes. *Nature Geoscience*, *10*(11), 816-821.
1203 https://works.bepress.com/wayne_wurtsbaugh/171/
1204
- 1205 Zhang, G., Yao, T., Xie, H., Qin, J., Ye, Q., Dai, Y., & Guo, R. (2014). Estimating surface
1206 temperature changes of lakes in the Tibetan Plateau using MODIS LST data. *Journal of*
1207 *Geophysical Research: Atmospheres*, *119*(14), 8552-8567.
1208 <https://doi.org/10.1002/2014JD021615>
1209
- 1210 Zhang, K., Kimball, J. S., & Running, S. W. (2016). A review of remote sensing based actual
1211 evapotranspiration estimation. *Wiley Interdisciplinary Reviews: Water*, *3*(6), 834-853.
1212
- 1213 Zhao, G., Li, Y., Zhou, L., & Gao, H. (2022). Evaporative water loss of 1.42 million global
1214 lakes. *Nature Communications*, *13*(1), 1-10. <https://doi.org/10.1038/s41467-022-31125-6>
1215
- 1216 Zucca, C., Middleton, N., Kang, U., & Liniger, H. (2021). Shrinking water bodies as hotspots of
1217 sand and dust storms: The role of land degradation and sustainable soil and water management.
1218 *Catena*, *207*, 105669.
1219